Acetylated Nanocellulose as a Reinforcement for Cellulose Acetate

Christopher Denton

Acetylated Nanocellulose as a Reinforcement for Cellulose Acetate

Christopher Denton

19019603

Dissertation for the partial fulfilment of the requirements of the degree

Master of Engineering (Chemical Engineering)

Supervisor

Prof. W. Focke

Co-supervisor

Dr. S. Ramjee

Department of Chemical Engineering

University of Pretoria

South Africa

CVD 800

2025-31-01

Acetylated Nanocellulose as a Reinforcement for Cellulose Acetate

Abstract

Current research has shown that the use of cellulose nanofibres (CNFs) can be used in the reinforcement of biodegradable plastics. Problems arise with certain polymers, such with cellulose acetate (CA), due to agglomeration of the nanofibres. Hydrogen bonds will form between cellulose fibres in a process called hornification which results in a poor-quality material and a waste of CNFs. It is thus necessary to modify the fibres such that they disperse into the CA matrix. The partial acetylation of CNFs can achieve this without destroying the fibrous network. However, there is a problem with this solution. The fibres when made can contain above 75 % water and have to remain in suspension or else irreversible agglomeration will occur. A recent discovery shows that xanthan gum can prevent this from happening by acting as a capping agent for the fibres preserving the fibrillated network during drying. Since the acetylation process can be affected by the presence of water this allows for a simple solvent swap to a solvent that does not affect the reaction. It is first necessary to demonstrate that acetylated CNFs will perform as expected without complicating the methodology.

CNF acetylation was carried out through the use of acetic anhydride after the nanocellulose solvent was swapped for acetic acid. Azeotropic distillation was used to ensure that as much water as possible is removed from the CNF. Acetylation was confirmed through FTIR analysis quantitatively compared the peaks from the double bonded oxygen in the acetyl group. In testing, various CNF contents and degrees of acetylation were used and in total sixteen different combinations were incorporated into CA films which were made through the solvent casting. All films were plasticized to 25 % with triacetin and solvent cast in watch glasses.

Microscopy images of the films revealed that acetylation of the CNF can reduce the agglomeration of the fibres by 400 % in the CA matrix, a clear indication that acetylation limits the hornification of the CNF. TEM imaging also shows the improved dispersion of the fibres

in deliberately collapsed CNF samples. Other experimental procedures showed that the modified films will have improved optical transparency and mechanical properties. UV-vis showed an acetylated CNF had 35 % less absorbance compared to its unmodified counterpart. The effect on the Youngs modulus from the CNF can also be increased by over 250 % through modification. Improvements in the tensile strength were limited due to CA already having a high tensile strength.

Effects on the rheology and viscosity of the modified CNF still need to be researched to gain a better understanding of the process on the materials shear thinning ability. This research has demonstrated that a biodegradable fibre reinforcement material can be used in certain polymers which previously posed a problem due to poor dispersion. This opens the door for more biodegradable polymers to be used in industry without the worry of the materials not being tough enough. There is potential for further development in this area, especially around polyhydroxyalkanoates, but the ability to minimise the fibre diameter is a big step in the right direction.

Keywords: Cellulose acetate, cellulose nanofibrils, acetylation, dispersion, fibre reinforcement

Acknowledgments

To the unwavering support of my parents who believed in me even when I could not, thank you, I would not be who I am today without them. Thank you to my brother and sister for teaching me all that I know. Thank you to my significant other who has helped me through all my years of study. Thank you to my Co-Supervisor, Dr. S. Ramjee, for his guidance. Thank you to my supervisor, Prof. W. Focke, who pushed me to ask the difficult questions and imparted to me the knowledge to find the answers. For the microscopy images, thank you Dr James Wesley-Smith. Thank you Dr Sabine Verryn for the XRD analysis and Ms. Lesego Temane for the tensile testing. A final thanks to PAMSA and Sappi for giving me the opportunity to be a part of something greater than myself.

Contents

List of Figures

List of Tables

Nomenclature

DS	Degree of substitution	–
2θ	Diffraction angle	°
λ	Wavelength	nm
Δm	Mass change of sample	g
P	Water vapour pressure difference across sample	kPa
Δt	Change in time	d
A	Area of sample	m^2
d	Diameter of fiber	m
E	Young's modulus	MPa
RH	Relative humidity	%
σ	Tensile strength	MPa
t	Thickness of sample	m
T_d	Decomposition temperature	°C
T_g	Glass transition temperature	°C
WVP	Water vapour permeability	$g\ m^{-1}\ d^{-1}\ kPa^{-1}$
$WVTR$	Water vapour transmission rate	$g\ m^{-2}\ d^{-1}$

1 Introduction

Throughout the past century, petroleum-based plastics have been used frivolously throughout every aspect of human life. This has led to major damage in ecological environments where nondegradable plastics interfere with and harm the fauna and flora. Biodegradable plastics are the solution to this global problem, however, they come with their own set of trials and tribulations. Cellulose acetate (CA), a polymer based on the cellulose fibres found in all plants, has the ability to replace a large portion of the plastic market but falls short in terms of certain mechanical properties(Nigam *et al*, 2022). Cellulose is one of the most abundant biodegradable, recyclable and naturally reoccurring materials. It is used by plants as a crucial part of the cellular structure, relying on the molecule to provide strength and rigidity to the plant (Somerville, 2006). In the new age of manufacturing turning away from the petroleum industry, due to the damage that it causes to the environment, it is as important as ever that the pulp and paper industry is capable of filling the market gap.

Cellulose is the main material in the pulp and paper industry but can be further refined to create new products in the form called nanocellulose (Dufresne, 2019). One of these products is Cellulose nanofibrils (CNFs) which can be produced through a number of different techniques. CNFs are highly refined cellulose fibres that have a diameter in the nanometer range and create interconnected webs. These webs have impressive tensile strength and can greatly improve the properties of a polymer matrix. This material has the additional benefits of being biodegradable and having a high surface area. Currently, the major uses of CNFs are in the cosmetic and construction industry where its shear thinning capability shines (Pandey, 2021; Rajendran *et al*, 2025). CNFs need to be suspended in a water solution, which only contain 8 % solid material, in order to avoid an irreversible process called hornification (Posada *et al*, 2020). In this process, as the material dries, strong hydrogen bonds form between the cellulose fibres which essentially revert the CNFs back into macro fibers. This can be avoided through certain drying methods however these methods are energy intensive (Nordenström *et al*, 2021).

Current research has shown that the incorporation of CNFs into CA can yield decent results with the use of a plasticizer, namely triacetin, but fail to maintain a high level of fibrillation of the cellulose fibers (Cindradewi *et al*, 2021). This comes from the dissimilarity between the two molecules. The CNFs will agglomerate to form a crystalized chain rather than attract to the acetyl groups of the CA. The proposed solution is to partly acetylate the CNFs in order to improve compatibility of the two chains (Ashori *et al*, 2014). This has shown great promise in certain other biodegradable polymers, such as PLA (Jamaluddin *et al*, 2019).

In order to acetylate the CNFs, acetic anhydride is used to replace the hydroxyl groups on the chain with the acetyl group (Sassi and Chanzy, 1995). Two problems arise here with the first in regard to the water content of CNFs. Acetic anhydride will first react with water to make acetic acid before it reacts with cellulose. The water has to be removed without collapsing the fibre network, this can be done through azeotropic distillation (Chien *et al*, 2004). Recent research has shown that a solvent swap can be done simply adding xanthan gum to the CNFs which maintains the network as it dries allowing a redispersion into acetic acid (Hoek *et al*, 2024). The second problem relates to the degree of acetylation of the cellulose fibres. This factor shows how many of the hydroxyl groups are replaced per monomer unit. If the acetic anhydride is allowed to attack the linking oxygen between the cellulose monomers, instead of the hydroxyl groups, the long fibrous chains will be shortened into undesirable cellulose nanocrystals (Miao *et al*, 2016).

If these factors are accurately controlled, they will lead to an acetylated fibrous material that can easily disperse into a CA matrix. This will result in improved tensile strength and Youngs modulus as well as a higher optical transparency.

2 Literature

2.1 Cellulose

Cellulose forms long crystallized strands in the cell walls of plants giving them high axial strength. Every species in the Plantae kingdom and even some from the Animalia kingdom, such as tunicates, make use of cellulose (Wertz *et al*, 2010: 21-24). It is such a common molecule that it has been discovered that humans can produce the substance from a disease called scleroderma however, the purest source of cellulose comes from the protective fibre that surrounds the cotton seed (French *et al*, 2000). This though does not contain the highest yield of cellulose per plant due to the extremely low density of the fluffy cotton thus, it is much better to acquire cellulose from dense wood. Hardwood naturally contains1 – 2 % more cellulose than softwood but requires more refining to split the fibres apart for use. The raw wood can be broken down into lignin, hemicellulose and the desirable cellulose products. The commercial industry for wood is one of the biggest in the world and is especially large in countries where lumber is used for housing. It was recorded in 2011 that around 31 % of the land area over Earth is covered in forests (Barbu, 2011). These wood reserves are vital to the world and have to be monitored carefully due to deforestation, especially in undeveloped areas. This comes from the utility of wood from being able to be used in housing and shelter to fuel sources and as the population rises so does the demand (Allen and Barnes, 1985).

The cellulose molecular structure is a D-anhydroglucopyranose unit connected by a β-1,4-glucosidic bond or more simply it is a β-1,4-glucan. These pyranose rings, a five-carbon and one-oxygen ring, take the shape of a chair conformation which has large implications for the stoichiometry in the macro chemistry of the molecule (Wertz *et al*, 2010: 21-24). This polyglucose falls under the category of polysaccharides which is defined as chains of carbohydrate molecules known as monosaccharides. This category incorporates starch which has a remarkably close relation to cellulose. The two molecules have a wide range of chemical similarities, both being made of glucose, but were differentiated due to their different

solubilities led to the discovery of cellulose having a trans glycosidic bond while starch a cis (Aspinall, 2014).

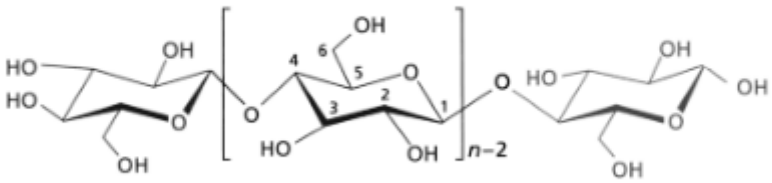

Figure 1: Cellulose Structure. Adapted from (Wertz *et al* 2020: 22)

The glucose monomer, chemical formula $C_6H_{12}O_6$, is considered one of the most basic energy sources and not only is found as a building block of cellulose and starch but in almost every cell of Animalia bodies. They form complex biochemical reactions allowing for the harvest of energy to be used throughout organisms (Navale and Paranjape, 2016). This energy, more commonly known as adenosine triphosphate (ATP), is a result of the breakdown of a glucose molecule in the glycolysis process to form pyruvate. Pyruvate is then further processed to reduce the molecule until all possible ATP has been recovered (Bertram *et al*, 2006). This demonstrates the high energy density that can be stored within a single molecule of glucose.

Cellulose is made from a β-D-glucopyranose which consists of an equatorial OH^- which results in the cellulose having the conformation of a flat ribbonlike structure (Wertz *et al*, 2010). This allows for the tight packing of the cellulose chains and an elevated degree of crystallinity. This leads to the creation of long fibres which create an interlocking web. An added effect is the reduced access to the OH^- ion which is concealed within the crystalline structure. The specific lattice structure that the cellulose forms, can be separated into types I, II, III, IV and amorphous (Nelson and O'Connor, 1964). The structure can be determined through infrared spectral analysis in the 850 – 1500 cm^{-1} with special interest given to type II and amorphous cellulose due to their similar peak ranges.

Native cellulose mainly consists of type I which has a complex crystal structure of two allomorphs, with one allomorph being more thermodynamically stable. Type II cellulose forms from the mercerization of cellulose either by dissolving, precipitation or treatment with an alkaline (Okano and Sarko, 1984). This is a more stable structure and thus an irreversible reaction. Further process of the cellulose by the inclusion of amines leads to the form of type

III cellulose which does not boast any major stability. Annealing of type III cellulose with glycerol produces the fourth lattice structure of cellulose. Both type III and IV have polymorph subclasses depending on the raw cellulose material (Wertz *et al*, 2010). The importance of the type of cellulose comes from when the cellulose is part of a reaction.

Cellulose, due to its wide availability and impressive mechanical properties leads it to be one of the most consumed raw materials throughout the world. Further on this point is the topic of highly refined cellulose in which the cellulose fibre is purified and milled to a smaller particle size. This refined product is called nanocellulose and has its own category of different types and morphologies (García Betancourt and Osorio-Aguilar, 2022). This is a very prominent topic as the process of refining the fibre gets better, and more research has to be done. An example of this can be the use of nanocellulose as a natural replacement for glass fibre (Venkatarajan and Athijayamani, 2021). As technology advances so does the possibility of this biodegradable material replacing non-renewable and environmentally damaging materials. In polymer science, this is an important topic as cellulose fibre-reinforced polymer composites have shown an impressive performance in mechanical properties. Examples of this have been in cements and plastics as well as the textile industry in which agricultural waste is used (Arbelaiz *et al*, 2023; Ragab *et al*, 2024). This along with the abundance and biocompatibility of nanocellulose make it a very desirable material (Trache *et al*, 2020).

2.2 Nanocellulose

Nanocellulose is split into three groups; bacterial cellulose (BC), cellulose nanocrystals (CNCs), and cellulose nanofibrils (CNFs) (Dufresne, 2019; Zinge and Kandasubramanian, 2020). Each type of nanocellulose has its own refining process and unique properties. BC, first reported in 1988, is made through an oxidative fermentation process of the cellulose by predominantly the *Acetobacter Xylinum* bacterium (Esa *et al*, 2014). To produce CNFs mechanical shearing is applied to break apart the fibrils while acid hydrolysis reacts with the amorphous region to break the fibre into CNCs (Dufresne, 2019).

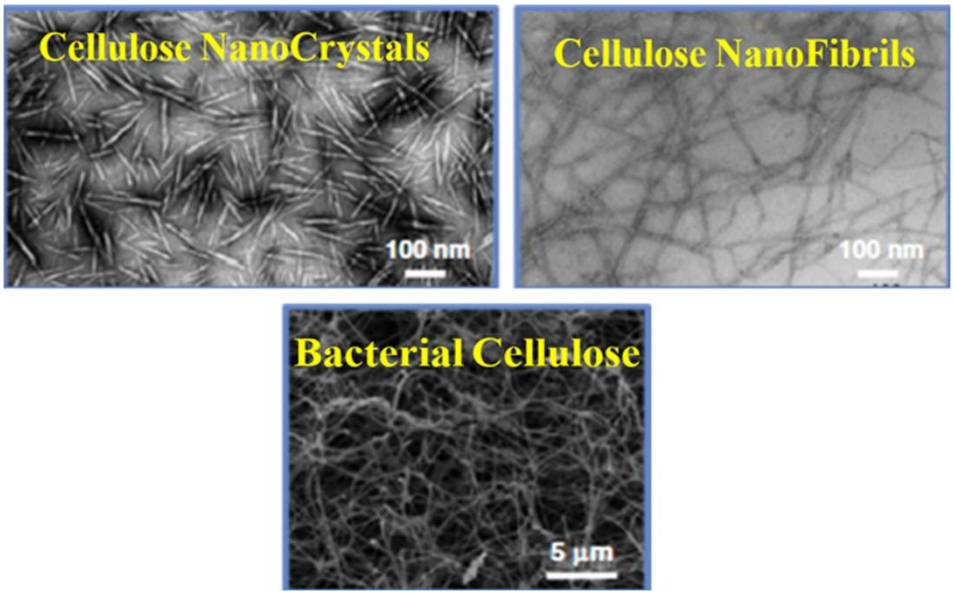

Figure 2: TEM Images of Nanocellulose. Reprinted from Nanocellulose based biodegradable polymers, (Zinge and Kandasubramanian, 2020), with permission from Elsevier.

The production process heavily influences the final morphology of the CNCs and comes down to the acid/alkaline hydrolysis of the cellulose, in most cases sulfuric acid is used as the hydrolyzing agent. Depending on the reaction time, concentration and temperature of the acid will determine the morphology of the CNCs (Qi *et al*, 2023). This process is capable of producing a broad variety of cellulose nanocrystals, 300 – 400 nm and 4 – 8 nm in length and height respectively, as well as cellulose nanospheres around 65 nm in diameter. Through other methods it is reported that a wider range of crystal sizes with diameters ranging from 4 – 55 nm and lengths in the range of 90 – 400 nm is possible (Zinge and Kandasubramanian, 2020). The special nature of CNCs is based on their high crystallinity, mechanical strength, biodegradability, barrier properties and high specific surface area which opens the material to a wide range of uses. Some of these uses include energy storage, matrix for printed circuit boards, organic aerogels, emulsion stabilizers, food additives, binders, biosensors, bio-imaging, biomimetic materials and reinforcement in polymer composites(Agate *et al*, 2018; Dufresne, 2019; Kim *et al*, 2019; Serpa *et al*, 2016; Trache *et al*, 2020).

With the focus on the reinforcement of polymer composite aspect of CNCs, it is vital to grasp the different morphologies of the crystals and the effects from them. Mentioned above was the acid hydrolysis method used in the production of CNCs. However, there are other hydrolyzing methods. Enzymatic hydrolysis makes use of fungi and bacteria that attack the cellulose fibres

to break it down into its crystal constituents. The drawback of this process is the time taken for the fungi and bacteria to break down the amorphous region of the cellulose, around 120 hours (Thompson *et al*, 2019). The final hydrolyzing method is via the use of subcritical water. Here a reactor containing cellulose is heated with water to above 120 ºC for 60 minutes with the pressure being maintained to prevent the water from boiling off. At this state there is enough energy to break down the long polymer into simple structures. This process has the advantage of not needing dangerous chemicals, thus being more environmentally healthy, and not requiring long processing times as in enzymatic hydrolysis (Thompson *et al*, 2019).

Regardless of the methodology used to make the CNCs, the separation and purification of the crystals remain the same across the board. CNCs have excellent dispersity in water therefore a large amount of water is used to wash the crystals followed by filtration(Nagarajan *et al*, 2021). In some cases, an ultrasonic bath is used to separate the CNCs from unreacted cellulose (Thompson *et al*, 2019).

BC has its biggest role in the medical and food industry. The interest in BC in the past 15 years has increased by 200 % which has come from a push from the pharmaceutical and biomedical fields (Fernandes *et al*, 2020). This is helped by the recent research into the production of BC through waste from agriculture, food, breweries, biorefineries, textile and pulp mills (Hussain *et al*, 2019). This has greatly lowered the cost of BC which makes it an extremely attractive substitute due to its wide range of properties. BC composites have also shown great performance in the use of skin, cartilage, artificial blood vessels, and bone (Moniri *et al*, 2017). The production process of BC is as simple as mixing cellulose and microorganisms and providing the right aerobic fermentation conditions. The optimization of the conditions is highly dependent on the microorganism with there also being a large selection of possible bacterium species (Fernandes *et al*, 2020). There have been 7 parameters that have been confirmed to have an effect in the fermentation of BC, as reported by (Fernandes *et al*, 2020), they are; inoculation ratio (1:15 to 1:10); substrate concentration; co-substrate concentration; inoculum age (3 to 30 days); dissolved oxygen (10 to 15 %); temperature (25 to 35 ºC) and the pH (3.5 to 7).

As with all nanocellulose materials, the final product is highly dependent on the type of raw cellulose used in the manufacturing process. This is especially true when it comes to BC, considering the fact that most inexpensive BC is made from waste, there is a large range of BC sizes and morphologies (Hussain *et al*, 2019). It is reported that the fibrils can have diameters

between 20 – 70 nm while the length can range from 300 nm to several µm. The morphologies can also range from large fibre bundles to flat sheet-like ribbons.

CNFs are a complex category of nanocellulose with its own subcategories. This comes from the fact that cellulose is already a fibre and therefore CNFs are a reduced version of the raw material. This leads the fibres to have their own set of mechanical properties, similar to that of the macromolecule but on the micro and nanoscale. The main difference between CNFs and other nanocellulose materials is the production method. Where the other materials are produced through a chemical reaction, the main process used to make CNFs is mechanical disintegration (Kargarzadeh *et al*, 2017). It is recommended to use hydrolysis to cut up the fibre, as done in the CNCs production, to impart new properties and improve the yield. The cellulose goes through a pre-treatment procedure to prepare the fibres for the mechanical shearing of the fibres. This is a chemical pretreatment but there are multiple methods listed as follows; 2,2,6,6–tetramethylpiperidine–1–oxyl (TEMPO) oxidation; carboxymethylation; phosphorylation; cationization; periodate oxidation and supercritical fluid (Yi *et al*, 2020). Both the hydrolysis and chemical treatment of the cellulose have a major effect on the overall yield of the CNFs. These processes are done to try and pull the cellulose molecule straight into the substrate as it is naturally intertwined from the high force of hydrogen bonding owing to the hydroxyl groups along the polymer. The chemicals mentioned above react with hydroxyl functional groups which reduces the forces of cohesion allowing the chains to be dispersed more easily. This is followed by the actual manufacturing process in which there are nine possible methods; high pressure homogenization; micro-jet; milling; ultrasonic treatment; low temperature pressing; steam explosion; electrospinning; solvent method and ionic liquid method (Yi *et al*, 2020).

It is important to understand the difference in each pre-treatment method of cellulose. This is due to the different mechanisms that are used as well as the functional groups that are attached to the fibre. TEMPO oxidization with the use of selectively oxidizes the primary hydroxyl group, substituting them with an aldehyde group particularly with the use of sodium, as the groups on the chain are hindered by the crystallinity of the cellulose leading to activity only on the surface of the crystalline region (Tahiri and Vignon, 2000). This process is still capable of improving the properties of the cellulose as well as reducing agglomeration problems. Carboxymethylation, similar to that of the TEMPO method, substitutes the hydroxyl group for a carboxyl. This creates a larger electrostatic force which pushes apart dehydrogenated fibrils. This process greatly improves the water solubility of the cellulose but comes at the cost of

using toxic chemicals and a complex reaction (Yi *et al*, 2020). It also damages the mechanical properties as well as makes the product opaque.

Phosphorylation adds an ionic charge with the help of a phosphate group replacing the hydrogen of a hydroxyl group. This improves the crosslinking of the cellulose (Kokol *et al*, 2015). This is a low-cost, non-toxic option with the added benefit of improving flame retardancy however it has been shown that too high of a concentration will lead to a reaction of the main chain in the amorphous region (Yi *et al*, 2020). Like phosphorylation, cationization makes use of a cation to improve fibrillation through electrostatic forces. The process has not received much attention the only real industrial uses have been for dyeing cotton with anionic dyes (Correia *et al*, 2020). Periodate oxidate differs from all the abovementioned cellulose pretreatment methods; instead of first reacting on the surface hydroxyl groups, the bond connecting the 2^{nd} and 3^{rd} carbons in the ring is broken and replaced with aldehydes to open up the ring. This does create free radicals which will reduce the celluloses degree of polymerization. The periodate pre-treatment is a very complex treatment method but it does produce interesting characteristics in the cellulose, such as improved flexibility; however, due to the expensive and toxic nature of this method, it is rarely seen in industry (Yi *et al*, 2020). The final pretreatment method, supercritical fluid technology, is an environmentally friendly method that is used throughout the cellulose industry. Supercritical CO_2 is used with major effects on the fibre, it is reported to smooth the fibres, improve surface area by making a finer network, increase the number of pores and break extensive bonding (Badgujar *et al*, 2021). It is also a useful method to introduce additives into the cellulose as well as purify the cellulose through the extraction (Yi *et al*, 2020).

The manufacturing process to mechanically create the CNFs is much simpler than the complex chemical pretreatment methods. The goal is to try to split the cellulose fibres from themselves taking the fibre from the microscale to the nanoscale. The most commonly used method is a high-pressure homogenization technique (Yi *et al*, 2020). Here pressures of above 100 MPa force cellulose through a small channel gap of 0.5 mm (Nakagaito and Yano, 2004). This is repeated multiple times, but the total number of passes is reliant on the channel gap as well as the pressure. This leads to a wide distribution of fibre sizes and lengths. A result of this is a multi-step process used to normalize the CNF distribution. An updated version of high-pressure homogenization makes use of an N-shaped or Y-shaped pathway through which the cellulose is forced at a pressure above 200 MPa at a speed of approximately 700 m/s, this is known as the micro-jet method (Ogura, 2021; Yi *et al*, 2020). This is more than twice the speed of sound

and the collisions between the fibres and the fibres with the channel wall is enough to cause fibrillation. The speed is high enough such that cavitations form from the jet injects, as these cavitations collapse they aid in dispersing the fibres (Ogura, 2021). Milling fibrillation, unlike the previous two methods, grinds the cellulose typically between two disks to shear the fibres. During this process, which can take up to 30 minutes, the disks are slowly moved closer together continuously squeezing the fibres. This is a fairly inefficient fibrillation method but requires less energy input at 1.38 kWh/kg (Wang and Zhu, 2016). The operation time of the process is indirectly proportional to the degree of polymerization and crystallization of the cellulose. Milling is a particularly useful fibrillation method as it is capable of handling high volumes of cellulose at one time. One non-invasive fibrillation method is the ultrasonic cavitation of the cellulose. High-frequency sound waves are sent into the cellulose dispersion and can cause pressures of above 500 atmospheres to burst the fibres apart (Yi *et al*, 2020). This burst comes from the collapse of cavitations caused by the high and low amplitudes which rapidly overlap and constructively interfere causing high- and low-pressure regions. Due to the explosive nature of this method, it is possible to break the nanocellulose into shorter fibrils, presumed from extensive bending (Redlinger-Pohn *et al*, 2022). An interesting method of fibrillation stems from the low temperature squeezing of cellulose. Here cellulose fibres are saturated with water or alkali and then frozen with liquid nitrogen, following this the crystals are sheared and impacted breaking apart the cellulose cells (Wang *et al*, 2007; Yi *et al*, 2020). This results in broken and fractured cells releasing the CNFs. A simpler fibrillation method, called steam explosion, creates CNFs by shooting high-pressure steam into cellulose fibres. This rips the cellulose out of the macro-fibres, purifying the cellulose in the process and increasing the degree of polymerization (Yi *et al*, 2020).

The final three fibrillation methods are grouped together due to their common property of creating a solution containing the cellulose before it is processed. The first, electrospinning, has the solution pushed through a needle injection port in the presence of a strong electric field. This creates a Taylor cone which forms the nanocellulose as the solution dries (Dizge *et al*, 2019). The advantages of this method are the wide range of varying fibre sizes that can be made while disadvantages include the difficulty of creating a solution to dissolve the cellulose (Yi *et al*, 2020). The second solvent method induces fibrillation in the solution by stirring it vigorously or with ultra sonification, this is helped with a non-solvent phase. Solvents like N-methyl morpholine oxide, commonly referred to as NMMO, need to be used in this process (El-Wakil *et al*, 2022). The final method uses either organic cations or anions to dissolve and

isolate the fibres, known as the ionic liquid method. This method has gained traction due to the recent research into green ionic solvents (Azimi *et al*, 2022). After the dissolution of the cellulose, the solution can be electro-spun or sprayed to form the CNFs. All of the solvent methods require complex chemical systems which are costly and can be toxic, therefore these methods are rarely used (Yi *et al*, 2020).

In terms of the characterization of nanocellulose, it is a fairly difficult task when it comes to fibrillation. Microfibrillated cellulose (MFC) can be seen as a semi-processed form of nanocellulose with its own properties and characteristics. When it was first reported in 1983 its main uses were stated to be as an emulsifier and suspending medium (Turbak *et al*, 1983). The production of MFC is similar to that of CNFs and mainly revolves around the mechanical separation of fibres to make smaller fibrils. The common methods for this are homogenization, fluidization and grinding (Spence *et al*, 2011). These are still energy-intensive methods but require less work than the nanofibrillation methods. The microfibrillation of cellulose does not require a pretreatment process as the fibres are still large enough such that the electrostatic forces aren't strong enough to keep the fibre agglomerated (Kumar *et al*, 2014). Both MFC and CNFs can improve the mechanical properties of a matrix, however the filler efficiency of MFC will show a better tensile strength but the better optical transparency and thermostability of CNF can lead it to be more desirable (Cheng *et al*, 2019). If incorporated into a film, the MFC composite is also reported to demonstrate higher resistance to oxygen and water vapour permeability.

In general terms, the higher the level of fibrillation of the cellulose, the higher the viscosity and surface area. There is also an increase in the distribution of types of morphology (Berto and Arantes, 2019). It is difficult to define the exact point at which a fibre is defined as nano- or micro-fibrillated therefore, it is commonly accepted that there is an overlap where a fibre can be referred to as either. MFC will contain fibres that are typically 20 to 400 nm in diameter and can be as long as a couple of micrometers while CNFs exist in the range of 5 to 100 nm in diameter and can as well be several micrometers long (Aulin *et al*, 2010; Chinga-Carrasco, 2011; Pääkkö *et al*, 2007; Saito *et al*, 2009). As the diameter decreases, the more singular fibres there will be which in turn leads to an exponential growth in the available surface area for the cellulose (Berto and Arantes, 2019). This does come from a much higher energy demand in order to produce the smaller fibre diameter.

MFC has been researched with regard to its role in composite materials. It is an older material compared to its more finely processed CNFs and also has some more desirable properties such as reduced agglomeration. Examples of composites including MFC are described below. Polyvinyl alcohol (PVOH) benefits from MFC by acting as a nucleating agent to help with the foaming of the composite (Zhao *et al*, 2015). Polylactic acid (PLA) is a prominent material that is known for its biodegradability and can have an improved tensile properties but requires a high loading of MFC, above 20 % (Huang *et al*, 2012). Acetylation can be used to decrease the polarity of the MFC and help with the dispersity of the fibres in the PLA matrix (Yetiş *et al*, 2020). A composite of gelatin and MFC can, along with the improved tensile strength, have better barrier properties. Here loadings of MFC can reach up to 25 %. The improvement in barrier properties is due to the cross-linking that occurs between the gelatin and MFC (Fadel *et al*, 2013). MFC has also shown its uses in the world of batteries as a binder for flexible electrodes. The web of fibres binds the graphite platelets allowing for flexibility of the electrodes that can also withstand the cyclic nature of the battery (Jabbour *et al*, 2010).

2.3 Cellulose modification

In some cases, it is necessary to modify the MFC to improve compatibility in composites. This usually comes through the use of functional groups that are attracted to the hydroxyl groups on the cellulose that are also capable of bonding to the matrix material. Such as the polybutylene succinate (PBS) and MFC composite where the MFC needs to be treated with acetylchloride (Zhou *et al*, 2016). This PBS composite is very reliant on the dispersion and alignment of the fibres in order to produce a material of high tensile strength, which can be done through melt stretch processing. The PLA composite can also benefit from a vinyl laurate modification of the MFC (Li *et al*, 2021). These two polymers, PBS and PLA, have recently been shown interest as a high mechanical strength material but comes at the cost of being brittle. Epoxidized MFC is used in the blend to aid in compatibility between the two polymers as well as be a reinforcement filler (He *et al*, 2020).

Great interest has been shown in the making of films with cellulose fibres as reinforcement. The strength and biodegradable nature of the cellulose leads it to be an excellent additive to films that are seen as green. One example of this is the incorporation of MFC and chitosan with

polypyrrole (PPy) (Gao *et al*, 2020). SEM imaging showed that the PPy chains coated the surface of the MFC and chitosan networks. This led to a reduction in the oxygen permeability of the film as well as increased hydrophobicity. This is a common property of MFC films (Syverud and Stenius, 2009). In some cases, it is better to use MFC instead of the more refined CNFs in the film composite due to the barrier properties (Kumar *et al*, 2014). The major industry this applies to is the food packing industry where it is important to keep the food separated from moisture and oxygen where it would otherwise begin to rot the produce. In some cases, both CNCs and MFC are used (Fotie *et al*, 2023). To be effective a thickness of 3 – 4 µm for MFC is required while CNCs require a third of the MFC thickness.

MFC and nanocellulose have a major challenge in the industry regarding the aggregation of the fibres. Nanocellulose materials are always processed in an aqueous suspension due to their hydrophilic structure. As the water content decreases the hydrogen bonding in the chains pulls themselves together collapsing the fine network structure (Peng *et al*, 2012a). This leads to multiple issues and essentially destroys the high surface area property of the cellulose. This aggregation is a common problem in the nanocellulose industry and can be irreversible leading to a ruined product (Ballesteros *et al*, 2022). There are methods which are employed to try and prevent this during drying. These methods are oven drying, freeze drying, spray drying and supercritical drying (Peng *et al*, 2012a).

Oven drying, being one of the simpler methods, requires the suspension to be heated up to remove the moisture. It has been found that the higher the temperature used in the drying process, the less dispersed and interconnected the fibres will be when they are resuspended (Silva *et al*, 2021). It is possible for MFC to recover its properties of mechanical strength if it is dried at room temperature or more simply put as air drying. However, multiple cycles of drying and redispersion will lead to a fall-off in quality. Freeze drying and supercritical drying are commonly used to expel water from cellulose fibres with supercritical drying having the benefit of avoiding the capillary action of the fibres (Mo *et al*, 2022). There is the downside of supercritical drying being more complex and costly thus, freeze drying is preferred in most practices. The method for supercritical drying requires a solvent exchange with ethanol which is dried with supercritical CO_2 to maintain the network structure. The method for freeze drying on the other hand is placing the suspension in an ultra-low temperature freezer, around – 50 °C, for as little as 24 hours(Mo *et al*, 2022). Spray drying can be an effective method to remove water from CNCs and large MFC particles but it has been shown that fibres that are in the scale of the CNFs range tend to agglomerate and destroy the fibre network (Peng *et al*, 2012b). This

highlights the essential problems when working with CNFs as at such sizes that the fibres are at, it is difficult to perform any modification or preservation without rendering the material useless.

The problem of drying nanocellulose summarized is as such, as the moisture content decreases hydrogen bonds form between the cellulose chains leading to the hornification of the fibres (Xu *et al*, 2022). The main factors that are focused on when trying to prevent this problem are steric hindrance and surface charge. There are multiple ways to change the surface charge, but they all revolve around altering the chemical structure of the polymer. Some of these modifications are oxidation, etherification, esterification, amidation, graft polymerization, acetylation, etc. (Chu *et al*, 2020). All these methods weaken the hydrogen bonding by reducing the number of available sites for the bonding to occur. The degree of substitution (DS) of the hydroxyl groups is thus a particularly important parameter. It is calculated as the number of substituted sites divided by the number of available sites. Aggregation also be prevented by keeping the fibres separate such that the hydrogen bonds cannot form (Posada *et al*, 2020). This can be done through the use of surfactants which when combined with nanocellulose place themselves in between the fibrils preventing hydrogen bonding. The properties of the nanocellulose can be adjusted depending on the anionic, cationic, nonionic or amphoteric surfactant used (Tardy *et al*, 2017). Due to the cellulose fibres having a slightly negative charge, anionic surfactants have a difficult time placing themselves between the fibres and require an electrolyte solution to overcome the electrostatic forces between the surfactant and cellulose (Sinquefield *et al*, 2020). Cationic surfactants on the other hand have strong interactions and have been shown to reduce the hydrophilicity of the fibrils, especially if they have been pretreated by TEMPO oxidization (Xhanari *et al*, 2011). This does depend on the selected cationic surfactant and in this case the TEMPO nanocellulose requires cetyltrimethylammonium bromide or hexadecyltrimethylammonium bromide. Nonionic surfactants are much less sensitive to pH and have peculiar temperature behaviour leading them to mainly be used in electrolytic solutions with low temperature fluctuations (Tardy *et al*, 2017). Amphoteric surfactants are special in the fact that their charge state depends on the pH of the solution. These surfactants are best used in the cosmetic industry for soaps and shampoos to improve lathering without causing irritation (Iwata and Shimada, 2012).

A parameter to measure the dispersity of nanocellulose is called the Zeta potential. This is the electric potential between two crystalline layers (Hamid *et al*, 2016). A suspension of nanocellulose is said to be well dispersed when the absolute Zeta potential is above 30 mV

(Chu *et al*, 2020). The treatment of MFC can drastically influence the Zeta potential from its unmodified value of -10 mV (Stenstad *et al*, 2008). This aligns with the fact that untreated nanocellulose will tend to agglomerate. This is shown in figure 3 where mass clumps of fibres can be seen with little to no separation between them.

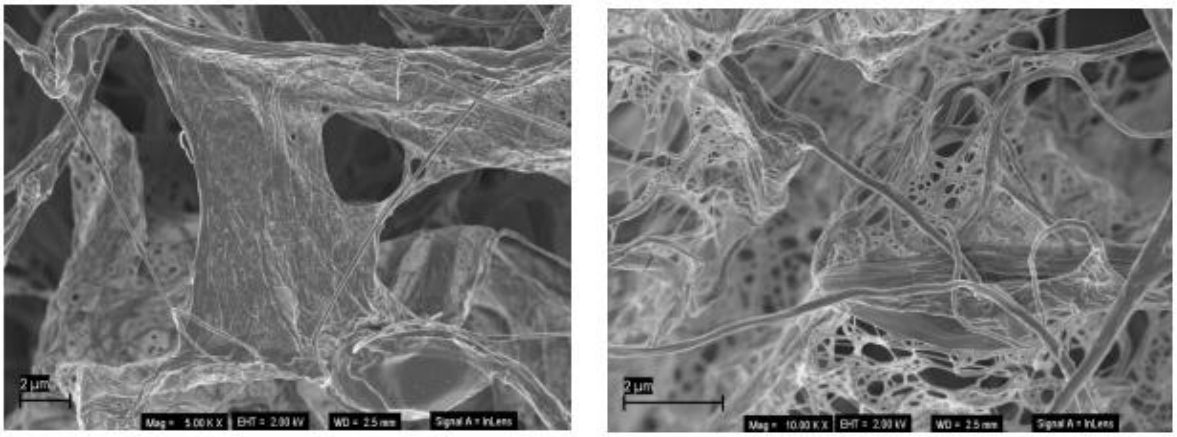

a) 5000 times magnification b) 10000 times magnification

Figure 3: SEM images of dried and redispersed nanocellulose. Used with permission from (Hoek *et al*, 2024).

2.4 Cellulose acetate

The acetylation of cellulose fibres led to the polymer known as cellulose acetate (CA) with the discovery being credited to Paul Schützenberger in 1865 (Rustemeyer, 2004). The experimental procedure was to heat cellulose with acetic anhydride in an isolated container. Cellulose triacetate, which is the fully acetylated version where each hydroxyl group is substituted, was first patented in 1894 by Cross and Bevan as an attempt to replace extremely dangerous nitrocellulose (Cross et al, 1895). The following years saw the potential of CA in uses such as photographic film, artificial silk and plastics however, due to the cost of the expensive raw materials, there was little commercial success (Rustemeyer, 2004). The procedure to make CA requires a large amount of acetic acid with acetic anhydride to acetylate the cellulose hydroxyl groups in the presence of a sulfuric acid catalyst (Braun et al, 2001). Partial acetylation of the

cellulose is possible forming the compounds cellulose diacetate and cellulose monoacetate. The DS for cellulose acetate has a maximum of three due to the three hydroxyl groups per glucose unit. Cellulose diacetate is referred to as CA has a DS of 2 – 2.5 and is soluble in acetone (Fischer *et al*, 2008). Above this DS the CA will be soluble in dichloromethane. This allows for easy purification and classification of CA.

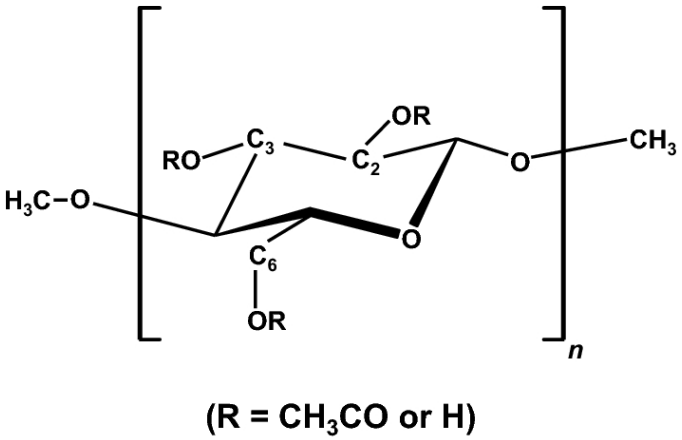

Figure 4: Structure of CA. Reprinted from All-atom molecular simulation study of cellulose acetate: amorphous structure and the dissolution of small molecule, (Matsuba *et al*, 2022), with permission from Springer Nature.

CA has a wide range of applications due to the numerous production methods. One of the oldest applications is the casting of films from a CA solution (Harris and Johnson, 1933). A more recent application that has received attraction due to the biodegradable nature of CA is the use in separation membranes (Vatanpour *et al*, 2022). A more classic use comes from the potential of CA to be spun into a fibre to be used in the textile industry (Fischer *et al*, 2008). It has also been used in many other areas from buttons and glasses frames to toys and cigarette filters (Puls *et al*, 2011). There are concerns over the environment when it comes to CA as compared to its unmodified counterpart. In order to degrade the polymer first needs to be deacetylated by enzymes or hydrolysis which can be done through UV wavelengths shorter than 280 nm. There is also the concern of sourcing the expensive and dangerous acetic anhydride which has no known natural sources (Cook, 1993). CA has raised many questions over the years about whether it can be seen as an eco-friendly material which comes from the lack of knowledge of the complicated environmental degradation of the polymer (Yadav and Hakkarainen, 2021).

CA has demonstrated its use throughout the years and the research done on the material is extensive. It has been found that CA with a DS just over 50 % leads to a suitable thermoplastic which can be easily processed (Ach, 1993). It is noted that CA has a pleasant texture which has led to be used as handles for many things such as tools and combs. One of the main production methods of CA products is through melt processing where the CA, usually in pellet form, is heated above the glass transition temperature and is forced into a desirable shape (Fischer *et al*, 2008). This requires heavy machinery such as screw extruders or injection molds which are used extensively throughout the polymer processing industry. The other production method, mentioned earlier, is the casting of a part or film through the evaporation of the solvent from the CA solution (Ferrarezi *et al*, 2013). Cellulose diacetate can dissolve in a number of solvents, but the best ones are acetone, acetic acid, dimethylacetamide and dimethylformamide. Water is a non-solvent for CA meaning that the incorporation of water into any CA solution will cause a phase inversion in which the homogenous mixture will separate into a liquid and solid phase (Kim *et al*, 2016). Water will also cause a problem in the acetylation of the cellulose as the acetic anhydride used to acetylize the cellulose will first react with the water in the cellulose to form acetic acid (Fritzler *et al*, 2014).

CA has very desirable properties, however the production of pure CA will lead to a product that is very brittle. This is where the use of plasticizers comes into play. Plasticizers are compounds that have the ability to place themselves between the chains of a polymer in the amorphous phase and allow for the chains to slide over each other reducing the intermolecular forces which would otherwise prevent them from doing so (Wypych, 2004). Due to the nature of polymers being long chains, it is possible with the right plasticizer to maintain the properties of the original polymer with the added benefits of the plasticizer. The benefits of a plasticizer include softening and making the material more pliable which can result in increased toughness; reduction in melt viscosity and temperature leading to easier processing; improved mold release from equipment; decrease in the glass transition temperature and many others which can be tailored to the desirable property of the polymer (Godwin, 2017; Wypych, 2004). Water can be argued to be the oldest plasticizer and was used by potters to soften clay, painters, woodworkers and by other people in many areas of life (Deanin, 1987). The number of commercial plasticizers has grown exponentially since the 1900s and can be attributed to the booming of the polymer industry around the same time.

Plasticizers for CA have been thoroughly researched and documented but over the past few decade, there has been more of a push for environmentally friendly plasticizers. These green

plasticizers have gained a large amount of attention, especially in areas where the polymer is in contact with people (Harmon and Otter, 2018). This comes from the fact that it is possible for an additive, such as a toxic plasticizer, to bloom out of a polymer as its crystallinity changes. Phthalates, which are considered to be some of the best plasticizers, hold true to this and there are multiple research articles documenting the harm that can be done to humans from being in contact with these compounds (Eales *et al*, 2022). There are many identified health issues that have been linked to phthalates. Diethyl phthalate, and its similar compounds, are considered to be the best plasticizer for CA and have been used frivolously throughout the years in multiple CA composites (Fordyce and Meyer, 1940). This led to the problem of finding a suitable substitute for the problematic plasticizers.

When selecting a plasticizer, it is important to consider all the property changes that are going to occur whether that be the physical strength of the biodegradability. A number of potential plasticizer groups are glycols, acetates and citrates (Erdmann *et al*, 2021). Although these are excellent plasticizers there is a point to be made for natural-based plasticizers. Lactic acid and octanoic acid have been put forward as potential green plasticizers and have shown some level of successful decrease in the glass transition temperature (Decroix *et al*, 2020). Unfortunately, these green plasticizers have a number of problems such as unmixing of the system and undesirable required concentrations. Glycerol and triethyl citrate can be considered as suitable plasticizers for CA films each with its benefits. Glycerol films demonstrate a high opacity drastically reducing light transmission while triethyl citrate shows good mechanical properties (Teixeira *et al*, 2021). Glyceryl triacetate, or more commonly known as triacetin, is the most comparable plasticizer to the phthalate groups and can significantly lower the glass transition temperature such that the brittle to ductile transition will occur around 60 ^{o}C for a plasticizer content of 20 % (Charvet *et al*, 2019).

Plasticizers, due to their nature of placing themselves between polymer chains, can also help with the dispersion of additives in a matrix. This can be done with a plasticizer that is electrostatically attracted to both the polymer base and the additive which in turn acts as a compatibilizer. This causes a synergistic effect in which the compatibilizer/plasticizer will reduce the crystallinity of the polymer resulting in an enhanced effect on the flexibility and elongation (Sofla *et al*, 2020). An example of this is the effect of glycerol and polyethylene glycol, both common plasticizers, having a five-time enhanced effect in a polyvinyl alcohol and chitosan system. This is also very prominent in PLA/ CA blends where the ring opening polymerization of grafted CA and PLA will act as a plasticizer (Xu *et al*, 2020).

2.5 Cellulose acetate composites

In terms of nanocellulose as an additive in CA, it is important to note all the issues faced when manufacturing a certain blend and the root cause of the problem. The main aspects regarding this are the immiscible nature of the two polymers and the resulting properties of the composite. Each nanocellulose category will be analysed with the point of interest being on CNFs. The reason for this comes from the advancements in the industry where the process of making nanofibres that have a smaller diameter and a longer length has led to an influx of potential uses (Omran *et al*, 2021). CNCs on the other hand have been well documented due to their existence in industry for the past few decades. This comes from the different production methods where CNCs use easy chemical methods and CNFs use complex mechanical methods to preserve the fibre length (Yi *et al*, 2020). This leads to the first issue of using CNFs as a reinforcing agent in CA.

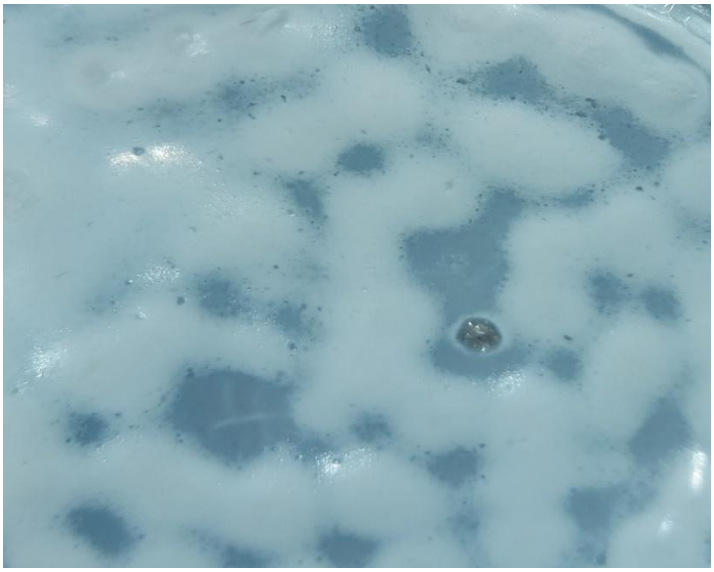

Figure 5: Agglomerations of unmodified CNFs in neat CA.

Figure 5 shows the phase inversion that occurs between the acetone solution of CA and the waterborne CNF solution (Abu-Zurayk *et al*, 2023). The work around for this problem is a simple solvent swap via azeotropic distillation (Chien *et al*, 2004). One of the main methods to improve compatibilization between CA and an additive is to acetylate the additive to a degree

such that it will induce a dipole force which will create electrostatic forces between the two compounds. This is done easily for CNCs as the process used to hydrolyze the cellulose fibre to make the nanocrystals can also be used to modify the cellulose by exchanging the hydroxyl groups for acetyl groups (Cheng *et al*, 2021). This process requires a mixture of sulfuric acid and acetic acid and produces the acetylated CNCs as a powder. The reason that this cannot be done for CNFs is because the sulfuric acid would react with the amorphous regions of the long fibre, and not the surface hydroxyls of the highly crystalline areas and would simply cut up the fibres to produce CNCs. The structure of the CNCs is naturally more chemical resistant whereas the fibrous network of the CNFs is good for mechanical properties, it is not robust in chemical stability (Rudie, 2017).

Another concern regarding the compatibilization of CNFs through acetylation is the solvent swap. CNFs have to remain hydrated or in a solution in order to prevent the collapse of the nanofibre web (Peng *et al*, 2012a). Throughout the production of CNFs water is used as the agent to suspend the fibres but this leads to a problem when it comes to acetylation. Acetic anhydride is used in the acetylation process to replace the hydroxyl groups but will also react with water in the system to produce acetic acid (Gold, 1948). The DS of the CNFs heavily affects the ability of the polymer to dissolve in specific solvents as well as the dispersity in the matrix. This DS has to be accurately controlled and this is done by limiting the amount of acetic anhydride added to the system such that a desirable DS is reached (Nabili *et al*, 2017). Therefore, any excess water in the system will react with any acetic anhydride in the system reducing the overall DS. The problem of removing the water while keeping the CNFs in suspension can be solved through the use of a centrifuge or a distillation (Ashori *et al*, 2014; Roman *et al*, 2021). These are both energy-intensive processes and require a large amount of preparation and run time in order to produce nanocellulose with minimal water content.

A recent discovery has been made which can completely avoid this problem of water removal. This discovery is in the use of xanthan gum as a capping agent to improve the dispersion of dried nanocellulose (Hoek *et al*, 2024). Xanthan gum is a hydrocolloid meaning it has the ability to absorb and hold onto moisture forming a gel-like substance. Due to its shear-thinning properties, it is often used in the culinary industry as a thickener for gravies, sauces, dressings, etc. but can also be found in other areas such as detergents, polishes and general coatings (Katzbauer, 1998). This shear-thinning property relates closely to the ability of CNFs to thicken and stabilize cosmetic products. This creates a synergistic effect of shear-thinning from the CNFs and xanthan (Blok *et al*, 2021). The main purpose of the xanthan gum is to prevent the

agglomeration of the fibres when the cellulose dries and then aid in spreading the fibres apart when redispersion is required, as seen figure 5. It is reported that the dried and redispersed solutions of CNFs and xanthan perform just as well as a never-dried solution (Hoek *et al*, 2024). It can thus be possible to theoreticize that instead of rehydrating the dried material with water, to use a solvent that CA is soluble in such as acetone. This will skip a large step of the production process and reduce the amount of chemicals needed to prepare the fibres.

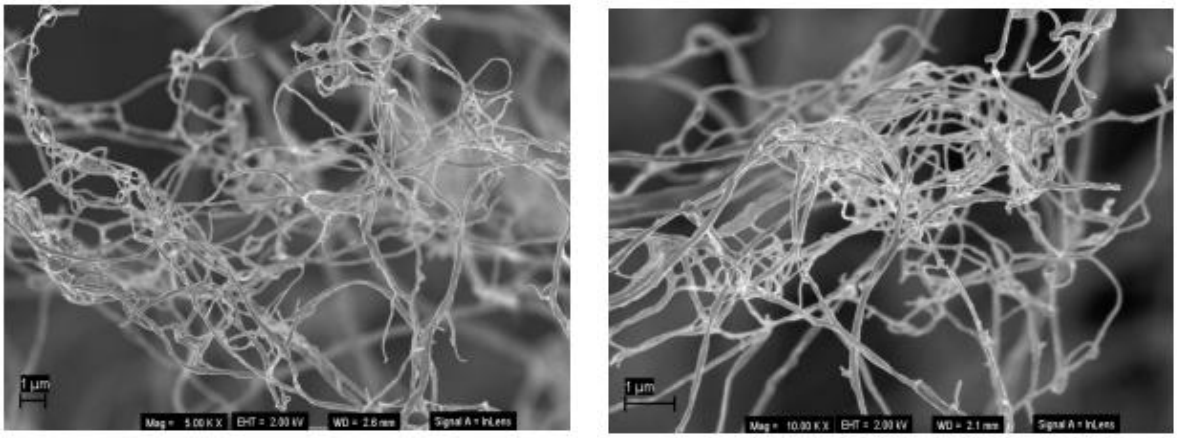

a) 5000 times magnification b) 10000 times magnification

Figure 6: SEM images of dried and redispersed nanocellulose with 15 % xanthan. Used with permission from (Hoek *et al*, 2024).

It has been shown that there is no conclusive evidence to say that the addition of xanthan gum to CNFs will affect the mechanical properties of the fibre with tensile testing proving so (Hoek *et al*, 2024). This comes from the fact that xanthan gum, also a polysaccharide, will have no problem in forming a fibrous web of interconnecting nanocellulose and xanthan. It is presumed high shear mixing between the two avoids any phase separation. Although this evidence is encouraging for the acetylation of dried CNFs there is also the concern of the acetylation of the xanthan gum chains leading to undesirable interactions in the polymer mixes (Endo *et al*, 2015). The incorporation of CNFs and xanthan into thermoplastic starch (TPS) has been shown to improve the mechanical strength of the biodegradable polymer (Hoek *et al*, 2024).

2.6 Overview

Lately, there has been a rise in research of CNFs being used as a tensile strengthening agent in polymer composites. The most prominent of these articles is researching the reinforcement of PLA with nanofibres (Tian *et al*, 2022). This incorporation does not only increase the strength but improves the elongation at break and impact strength. A fairly low loading of CNFs is reported and can double a polymer's strength properties at weight loadings as low as 4 %. There has also been research done into the effect that different surface modifications will have on the polymer (Zaaba *et al*, 2021). Research has stated that the modification of functional groups on the cellulose fibre can increase the interfacial bonding between the PLA and CNFs. However, in a composite of polyvinyl acetate (PVA) or polyvinyl alcohol (PVOH) with CNFs, no modification is needed as both waterborne substances can mix easily (Chaabouni and Boufi, 2017).

The research in CNFs reinforced polymers is still a fairly new topic however the push for use in biodegradable polymers like CA is still discovering its full potential. A dispersion of CNFs in CA can be improved by the use of N-methyl-2-pyrrolidone and certain other solvents however, this does come with its own cost and production methods and thus is not viable for large scale production (Cindradewi *et al*, 2021). There have been publications on the use of surface modification to improve the properties of MFC and CA blend (Lu and Drzal, 2010). However, these publications do not work with smaller fibre diameters which would be destroyed in the current surface modification processes.

Pass results have shown that the incorporation of CNFs can increase the tensile strength from 5.4 MPa to 23.0 MPa in TPS and from 47.0 MPa to 52.0 MPa in PLA (Hoek *et al*, 2024; Hoek *et al*, 2023; Wang *et al*, 2020). This data backs the fact that CNF reinforced polymer composites have the potential to be the material of a zero-carbon future.

3 Experimental

3.1 Materials

Cellulose diacetate batch number HH20191010 from Haihang Industry Co. was used in the making of all films. Sappi supplied the CNF in the form of Valida S191C 8 % Batch SB-20-0126-01 and was measured to have a solids content of 8.2 %. Acetic anhydride, with a purity ≥ 98.5 %, was sourced from Emsure through Merk. 99 % Triacetin from Aldrich was used as the plasticizer for all film making. Platinum line acetone, acetic acid and sulphuric acid were purchased from Acechem.

3.2 Methods

3.2.1 Acetylation of cellulose nanofibres

The modification of the CNF was done in batch processes and were stored at a temperature of 4 °C. Each batch followed the same process except for the differing amounts of acetic anhydride. This amount relates to the DS of the CNF, more specifically, on average how many hydroxyl groups of the cellulose have been replaced by acetyl groups. Four different DS values were chosen being 0, 0.5, 1 and 1.5.

First, 30 g of the raw CNF was weighed out in a 250 mL beaker followed by 150 mL of acetic acid. The mixture was initially mixed by hand with a spatula for a minute followed by mixing with a Silverson L4RT high shear mixer at 2000 rpm for 2 min. An azeotropic distillation setup was then used with the heating element gradually increasing to a temperature of 120 °C and magnetic stirring set at a speed of 500 rpm. The mixture was poured into the round bottom flask and the heating element turned on. The setup was run until the temperature stabilized, at which point 50 mL of additional acetic acid was added to the round bottom flask. The distillation was then run for a further 20 minutes. A sample was put aside to be used in the

analytical section as well as to confirm the percentage solids. The remainder of the paste was then stored and used as the base material for the acetylation.

Each acetylation was done using 20 g of the base material, which with the weight percentage known, calculated the amount of pure CNF withing the 20 g. The material was placed in a 250 mL beaker with 100 mL of acetic acid and then high shear mixed at 2000 rpm for 1 min. A large magnetic stir bar was added, and the beaker placed on a hot plate set to 60 ^{o}C and 400 rpm. Once the temperature was reached, 50 µL of sulphuric acid was added with 10 minutes given to allow it to thoroughly disperse. The precise amount of acetic anhydride for the batch was calculated with a 5 % excess and then added to the beaker. The solution was then covered and given 4 hours to react which afterwards 50 mL of deionized water was slowly poured into the mixture to prevent any further reaction. This amount is low enough to not cause a phase separation in the cellulose acetate film.

The solution was then vacuum filtered and washed with acetic acid before being labeled and stored at 4 ^{o}C. A small amount was weighed and put aside and once dried could be used to calculate the weight percentage of each acetylated paste. These values would range from 4 % – 6 %.

3.2.2 Cellulose acetate film preparation

All films were made using the film casting method with triacetin used as a plasticizer. For each of the acetylated pastes, four films were made with varying amounts of CNF, namely 2 %, 5 %, 10 % and 15 %. These percentages refer to a sole CA / CNF mixture excluding the plasticizer. The naming of the films is shown in Table 1, note the control film which contains no CNF is labelled as “Pure” throughout the report. To make the films first the correct amount of paste was weighed in a beaker such that the dried CNF is equivalent to the corresponding percentage of 1 g. 50 mL of acetone is then added and stirred by hand for 30 seconds to loosen the paste before being mixed in the Silverson L4RT at 1500 rpm for 2 min. Once it was confirmed that there were no CNF lumps remaining, CA was added such as to bring the dry weight of the solution to 1 g. At this stage 0.33 g of triacetin add equivalent to 25 % of the final dried solution percentage.

Table 1: Nomenclature of films used in testing.

Degree of Substitution	CNF Content (%) 2	5	10	15
0	C2DS0	C5DS0	C10DS0	C15DS0
0.5	C2DS0.5	C5DS0.5	C10DS0.5	C15DS0.5
1	C2DS1	C5DS1	C10DS1	C15DS1
1.5	C2DS1.5	C5DS1.5	C10DS1.5	C15DS1.5

The solution was then well mixed on the Silverson at 2500 rpm for 3 min to insure a good dispersion of the CNF across all the samples. During this mixing, air is pulled into the solution due to the increased viscosity of the CNF and CA. To deal with the trapped air a vacuum chamber is used. Each solution goes through three cycles of depressurizing the chamber to 0.4 bara where it is left for 1 min then slowly repressurized back to atmospheric pressure. The mixture is then poured into an 80 mm diameter petri dish and left overnight in a fume hood to allow the acetone to evaporate. For the higher percentage CNF films, the lids of the petri dishes were used to half cover the films to slow the evaporation otherwise the rapid drying would cause the films to warp.

The films were removed from the petri dishes and had the edges trimmed. Each mixture would result in a film with a thickness of approximately 110 µm. They were then labeled and then placed in an airtight box to later allow for conditioning. A saturated NaCl solution was made and placed in the box to condition the films which stored at a temperature of 20 ºC led to a relative humidity (RH) of 76 % (Winston and Bates, 1960). This is a high humidity but, due to the fibres increasing the stiffness, will allow the films to perform more consistently throughout the testing phase.

3.3 Analytical techniques

3.3.1 Fourier transform infrared spectroscopy

Fourier transform infrared spectroscopy (FTIR) was used to confirm the acetylation of the CNF as well as quantitatively check the DS of each paste. A Perkin Elmer Spectrum 100 FTIR Spectrometer was used with an attenuated total reflectance (ATR) attachment to allow for consistency between scans. Scans were taken on a range of 4000 cm^{-1} to 650 cm^{-1} at a resolution of 4 cm^{-1} and a total of 32 scans per run. The scans were baseline corrected and rescaled before being used in the calculation to confirm the DS.

3.3.2 Ultraviolet-visible spectroscopy

Alongside the FTIR analysis, UV-Vis was done to confirm the effect of the acetylation of the CNF in the CA films. A Hitachi U-3900 Spectrophotometer with an integrating sphere was used to measure the absorbance of the films from 200 nm to 600 nm. Cellulose has an absorbance peak around 280 nm at which the absorbances will be used in calculations. Spectragryph v1.2.16.1 was used to smooth; baseline correct and rescale the spectra.

3.3.3 Water vapour permeability

To determine if the addition of the CNF to the films affected the water vapour permeability (WVP), an ASTM E96 test was conducted with the desiccator setup. Cobalt chloride was used as the desiccant. After the desiccator was conditioned with a salt solution for a day, 3d printed cups were filled with the salt solution and sealed with circular cut pieces of film. The cups were weighed each day until they started to plateau. The following equations were used to calculate the WVP of the samples (Cazón Díaz *et al*, 2022).

$$WVTR = \frac{\Delta m}{A\Delta t}$$

$$Permeance = \frac{WVTR}{\Delta P}$$

$$WVP = Permeance \cdot thickness$$

3.3.4 Differential scanning calorimetry

A Perkin Elmer Differential Scanning Calorimeter (DSC) 4000 was used to determine the melting point of the films. 5 mg of each film was cut into pieces and placed in an aluminium pan which was then sealed and pierced with a pin. The test was run for only DS = 1, as well as the pure CA, since initial testing showed no real variance between samples with different DS. Samples were first cycled from 50 ºC to 150 ^{O}C at a rate of 20 ºC/min to act as a pre-treatment which is followed by heating from 50 ºC to 280 ºC at a rate of 10 ºC/min.

3.3.5 Dynamic mechanical analysis

The glass transition temperature (T_g) is determined through the Dynamic Mechanical Analysis (DMA) of the films. The 0.1 mm thick films were not stiff enough to register on the Perkin Elmer DMA 8000 and as a result aluminium sleeves were used to house the films. This meant that storage modulus $E^{'}$ would not convey any useful information, however, the tan delta curves from the DMA would still be valid to confirm the T_g. The tests were run from 30 ºC to 180 ºC at a rate of 2 ºC/min and a frequency of 1 Hz with a strain factor of 1.684.

3.3.6 Thermogravimetric Analysis

Thermogravimetric Analysis (TGA), which is used to measure the weight change during the decomposition of a material, was done on a TA instruments TGA 5500. Only the DS = 1

samples were measured as the difference acetylation of the films would not lead to a large difference in the decomposition and is not the focus (Carvalho *et al*, 2019). The pure CA as well as the neat CNF paste were also measured in order to be able to see the effect of mixing these two components. Aluminium oxide (Al_2O_3) crucibles on high temperature platinum pans were first tared and then filled with 5 mg of cut up pieces of film. The samples were heated at a rate of 20 ºC/min from 30 ºC to 800 ºC in a nitrogen (N_2) atmosphere.

3.3.7 X-ray diffraction

The X-ray diffraction (XRD) is a vital test to see firstly what the impact of the acetylation was on the CNF and secondly the crystallinity of the CA with the incorporation of the acetylated CNF paste. Therefore, all the CNF samples were tested and the DS = 1 films. The diffractograms were captured on a Malvern Panalytical Aeris diffractometer with a PIXcel detector and fixed slits. Fe-filtered Co-Kα radiation (λ = 0.1789 nm) was used with a back-loading preparation and zero background holder method. Scans were taken from 5 º to 80 º 2Θ at 0.02 º/s. 40 kV and 7.5 mA were the generator settings used across all testing.

3.3.8 Transmission electron microscopy

CNF were made visible in Transmission Electron Microscopy (TEM) by negative staining. 0.5 % Uranyl Acetate was used as the stain of choice. Pure CNF was allowed to dry for the imaging resulting in the fibre network collapsing. A 5 µL drop of diluted CNF solution was placed on one side of a carbon-coated TEM grid. After 30 seconds the grid was placed CNF side down on a 5 µL of uranyl acetate followed by removing excess liquid by bringing the grid into contact with filter paper. The grids were allowed to air dry and were then imaged on a JOEL JEM 1400 Flash TEM at 100 kV.

3.3.9 Scanning electron microscopy

Scanning Electron Microscopy (SEM) was used in complementary to the TEM imaging more specifically, to see if the change in CA films with the addition of CNF. Cross sectioned surfaces of the films were imaged using a JEOL IT200 at 5 kV.

3.3.10 Light microscopy

In order to get a better understanding alongside the images from the TEM and SEM, a Motic DMB1-223 light microscope was used to image the films. The microscope was calibrated, and images were taken at 1000 X magnification with immersion oil used on the films. Images were captured and edited on MotiConnect v1.0.1.9.

3.3.11 Mechanical testing

One of the most important factor in the development of this film is to prove that the addition of acetylated CNF will improve the quality of the film, specifically improve the Youngs modulus without compromising the maximum tensile strength. This was found through the ASTM D882-18 standard, which is a common tensile testing method for films with a thickness of 1 mm or less. An Instron 5966 universal testing system was used at an extension rate of 10 mm/min and a grip separation of 40 mm. In order to improve in consistency across the test, a custom dog-bone punch was 3D printed licensed as Print-A-Punch (Nelson *et al*, 2020). This punch had the blades replaced every five samples to maintain a consistent cut throughout the manufacturing of the test samples. Each sample had seven dog-bone blanks with the film thickness measured at three points and averaged.

4 Results and Discussion

4.1 Characterisation of acetylated cellulose nanofibres

4.1.1 Fourier transform infrared spectroscopy

Pure CNF spectrum is shown in Figure 7. It has been shown that the absence of a peak at 1111 cm^{-1} and the bands at 1158 cm^{-1} and 900 cm^{-1} indicated that the CNF is largely amorphous (Hoek *et al*, 2024). This comes from the fact that the fibrous CNF network is in direct opposition to the crystallinity of the nanocellulose. Relative FTIR bands are shown in Table 2 with special notice being taken to the C=O bond (Li *et al*, 2019; Nelson and O'Connor, 1964).

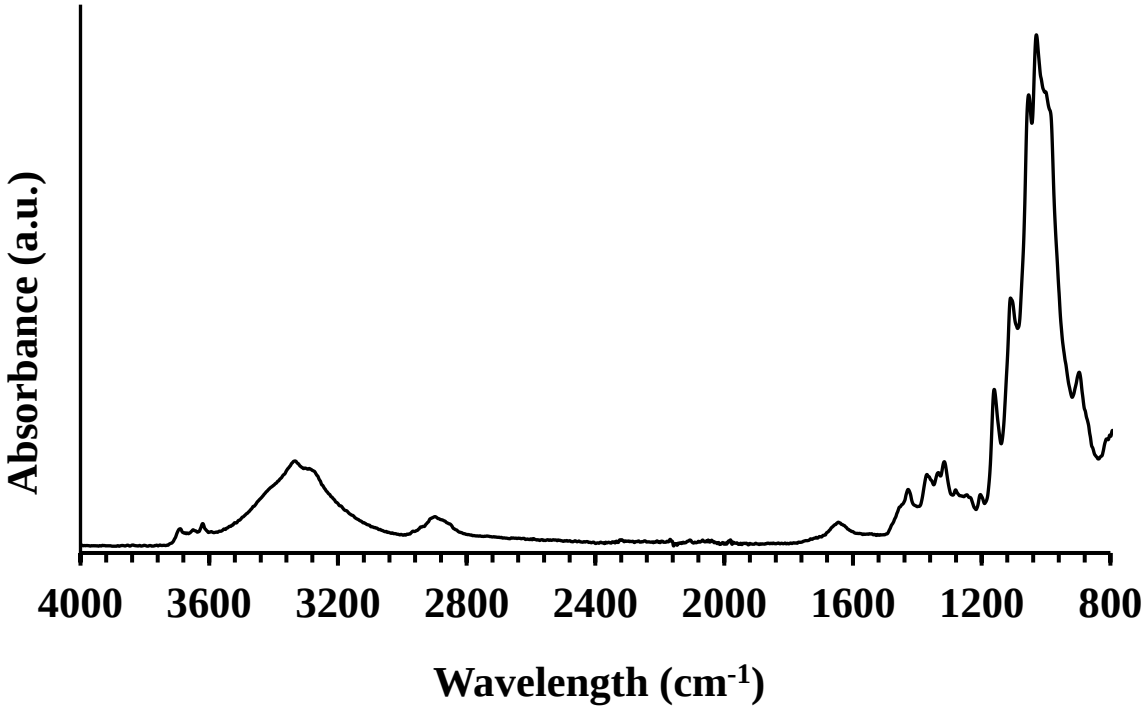

Figure 7: FTIR of CNF with DS = 0.

Table 2: FTIR bands of CNF(Li et al, 2019; Nelson and O'Connor, 1964)

Band	Wavenumber (cm^{-1})	Bond Type
O-H	3337	Stretching
C-H	2901	Stretching
C=O	1744	Stretching
H_2O	1646	O-H Vibration
CH_2	1428	Scissoring
O-C-H	1317	Bending
C-O-C	1158	Stretching
C-O	1030	Stretching

On the unit monomer of cellulose there are three hydroxyl groups which have the potential to be replaced. As the hydroxyl groups are replaced the polymer, although still biodegradable, will become more resistant to decomposing. It is therefore the case to try and minimise the DS without compromising the results. In order to determine the DS, the FTIR spectra have to be related to each other. By using pure unacetylated CNF as one control and cellulose diacetate, purchased from Haihang Industry Co., as the second a scale can be set which can be used to calculate the DS of the modified CNF. To quantitatively confirm the DS of the CNF, the FTIR spectra of the modified pastes is analysed. The C=O band which peaks around 1744 cm^{-1} is used in this case since this bond is solely found in the acetyl group which replaces the hydroxyl group during acetylation. Since the absorbance of the spectra is dependent on the contact of the substance with the equipment, the measurements have to be scaled such that the area under a common band is the same for all spectra. For this reason, the C-O-C band was used as the reference as it remains unchanged throughout all CNF sample preparations (Li *et al*, 2019). Figure 8 shows a compound graph of the spectra used in this calculation with the arrow indicating the increasing absorbance of the C=O bond.

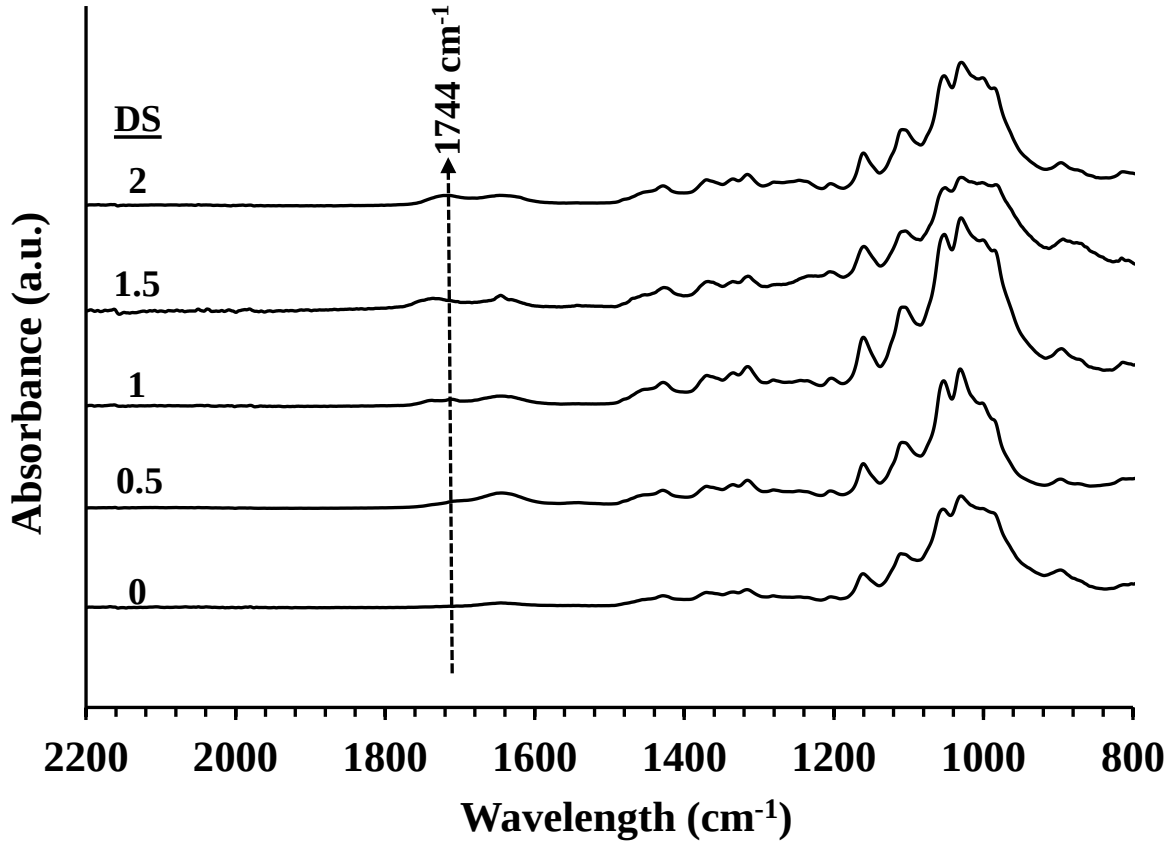

Figure 8: FTIR spectra of CNF at various DS.

Due to the absorbance of bound water being close to that of the acetyl group, it is important to show there are discernible bands. Figure 9 shows an enlarged section of the DS = 2 and the DS = 0 samples as well as the subtraction of the one from the other. It can clearly be seen that the subtraction shows a precise band for the acetyl group. The relative area for each spectra can be calculated by taking the area from 1718 cm^{-1} to 1756 cm^{-1} divided by the area from the C-O-C band, taken from 1140 cm^{-1} to 1176 cm^{-1}. This number is multiplied by the area from the acetyl group of the DS = 2 sample. The DS for each sample is now correctly scaled and by subtracting the value for DS = 0 for each sample, as this can be seen as background noise, we are left with the corrected DS. The corrected DS is plotted versus the expected values in Figure 10, the trendline as well as the R-squared value are displayed. With an R-squared value of 0.9853, each CNF sample DS is well within the expected range and can be used further in experimentation. As a secondary confirmation, each corrected DS, excluding DS = 0, is divided by the target DS to get a ratio close to 1. The relative standard deviation is taken across these ratios and results in a value of 12.37 %. This value is higher than expected, however due to the deviation existing

over a mean of 1.09 and a high R-squared value, it is still an acceptable confidence interval to go forward with in the experimentation (González and Herrador, 2007). A table displaying the above calculations is listed in Appendix A.

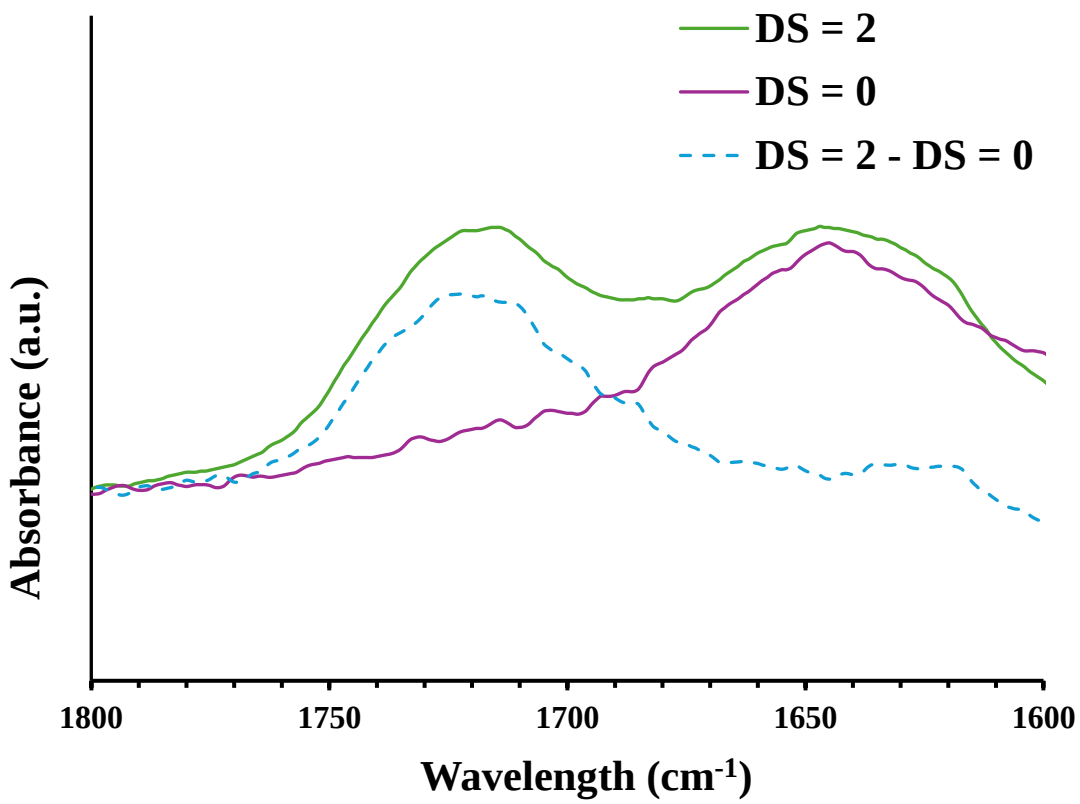

Figure 9: FTIR graphs showing discernible bands.

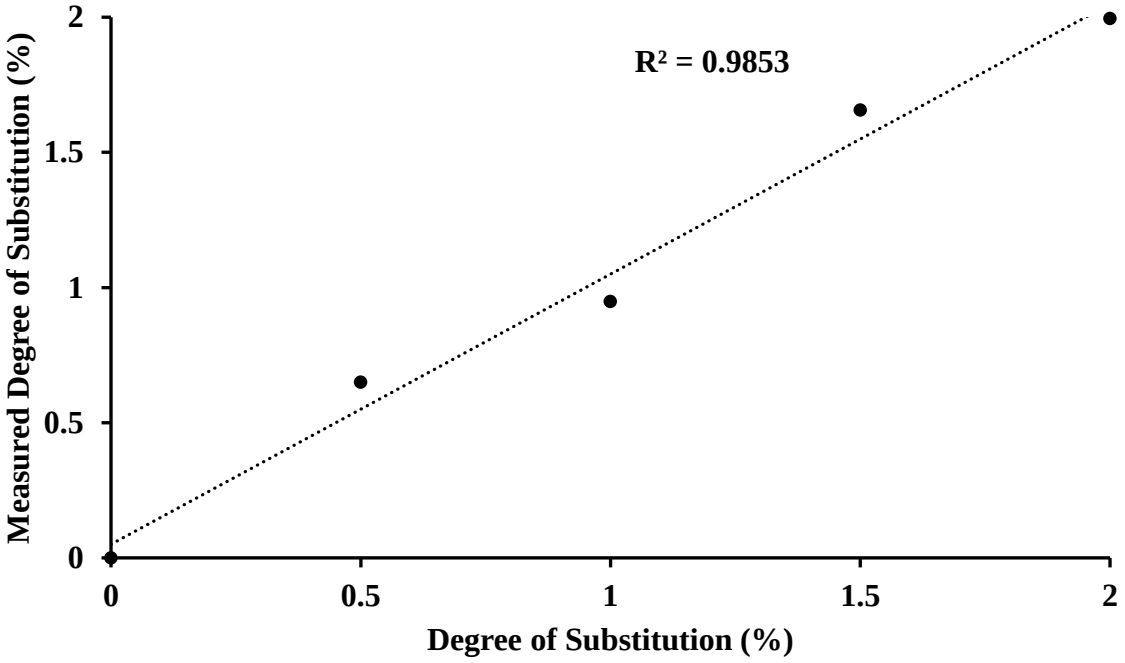

Figure 10: Plot of measured DS versus expected value.

4.1.2 X-ray diffraction

Crystallinity plays an important role in the physical characteristics of a material. It will determine many aspects such as thermal degradation hardness and density as well as give key information for the mathematical and spatial design of a system (Ward, 1950). In terms of CNF, the long polymer chains reflect a high crystallinity which would make sense due to their tougher characteristics compared to more amorphous BC (Setyaningsih *et al*, 2018).

Figure 11**:** XRD of CNF at Different DS shows the XRD of the plain CNF pastes with their differing DS. The pattern in all measurements show a shift to the right from the known XRD for cellulose. The main peak which is around 28º would seem to align with type I_{β} cellulose which is known to have a peak closer to 26º (Kim *et al*, 2013). The shift is attributed to the process of acetylation, namely the solvent swap section which all CNF samples were subject to (Shaaban, 2015). The important thing to note here though is that the DS has not majorly

affected the crystallinity, and by extent the integrity of the fibre's, as all graphs exist around the unacetylated DS = 0 CNF.

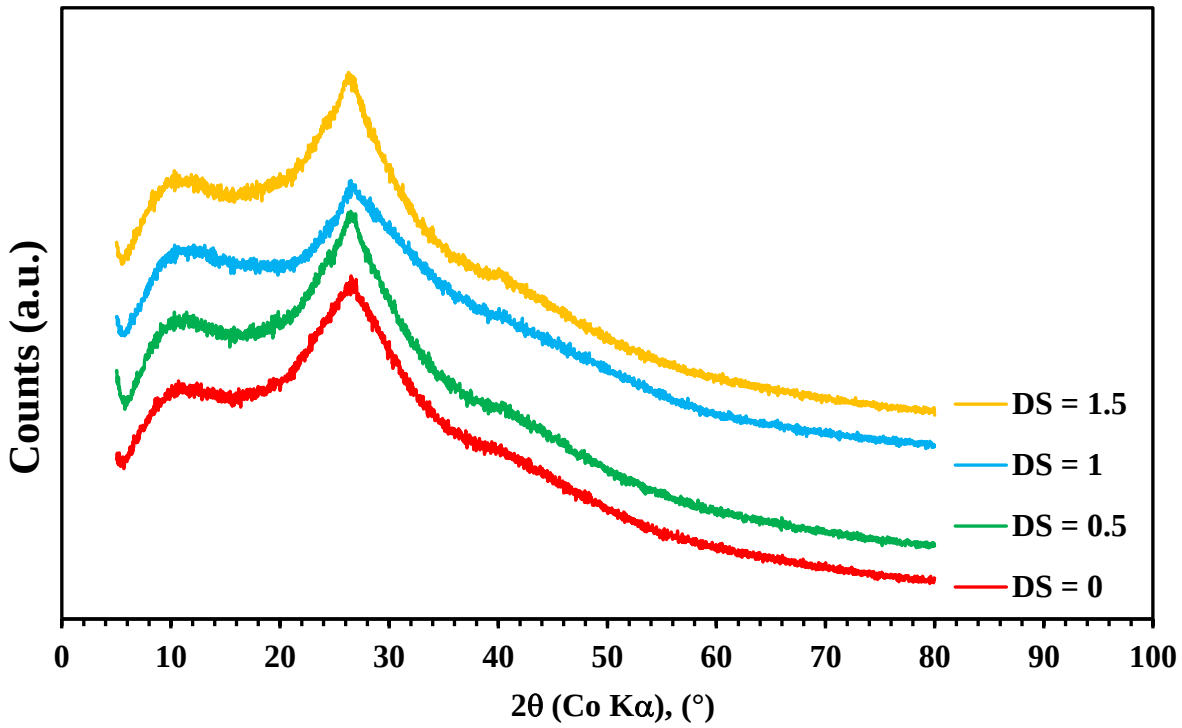

Figure 11: XRD of CNF at Different DS.

4.1.3 Transmission electron microscopy

One of the main goals of this research is to confirm that the acetylation of CNF has had an effect on the hornification, or the agglomeration, of the fibres while not shortening them. TEM microscopy was the ideal choice for this as it would simply show a flat 2D picture of the CNF pastes that can be easily compared between one another. All TEM images below are of fully dried CNF which will result in the hornification of the fibres (Peng *et al*, 2012a). Thus, the images themselves are not very impressive but still give an insight into the effects of the hornification process.

Due to the negative staining process, one can see the fibre bundles as well as the network resulting from it. As the stain is added it will attach itself to an available surface. If there is a high degree of agglomeration, the stain will not be able to penetrate into the bundle which will result in the TEM showing more of a grey area with low contrast. This is seen in Figure 12

where it is hard to differentiate between fibres in the bundle. Compared to the other figures with a DS greater than 0 there is a clear difference in the ability to see the alternating light and dark regions within the strands. This indicates that the stain was able to go in between the fibre strands due to less agglomeration.

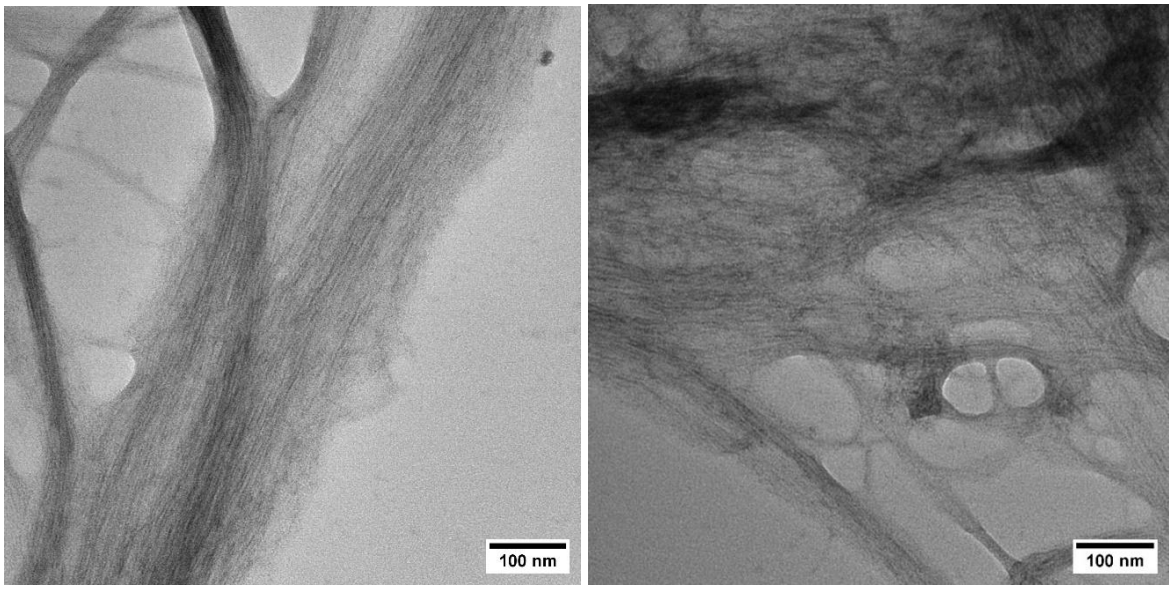

Figure 12: TEM image of CNF with DS = 0.

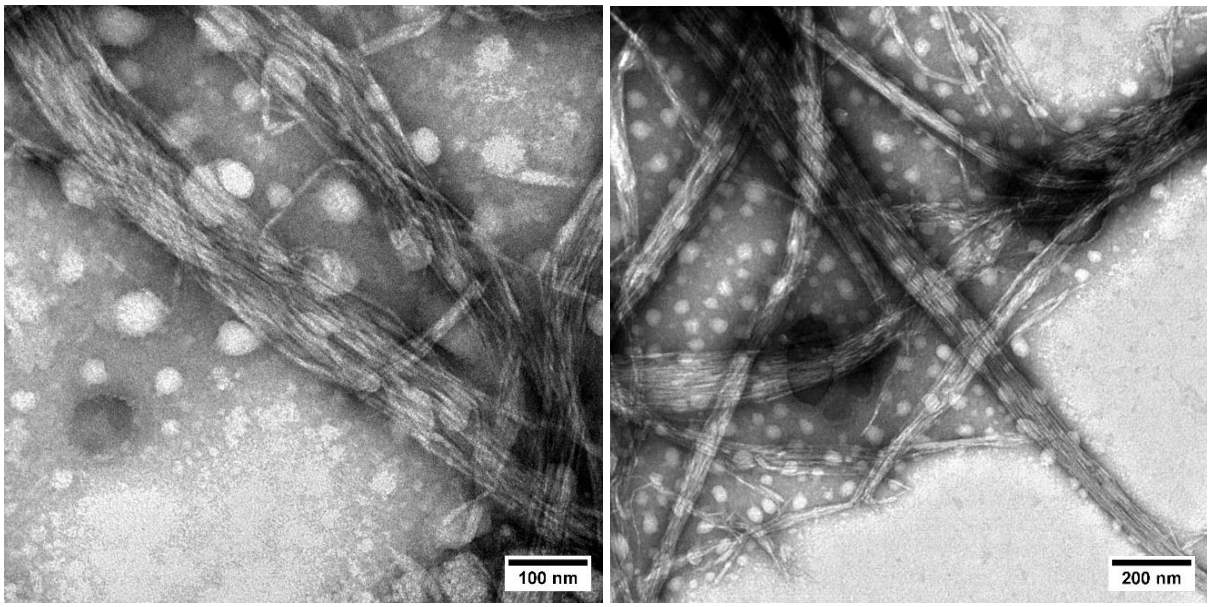

Figure 13: TEM image of CNF with DS = 0.5.

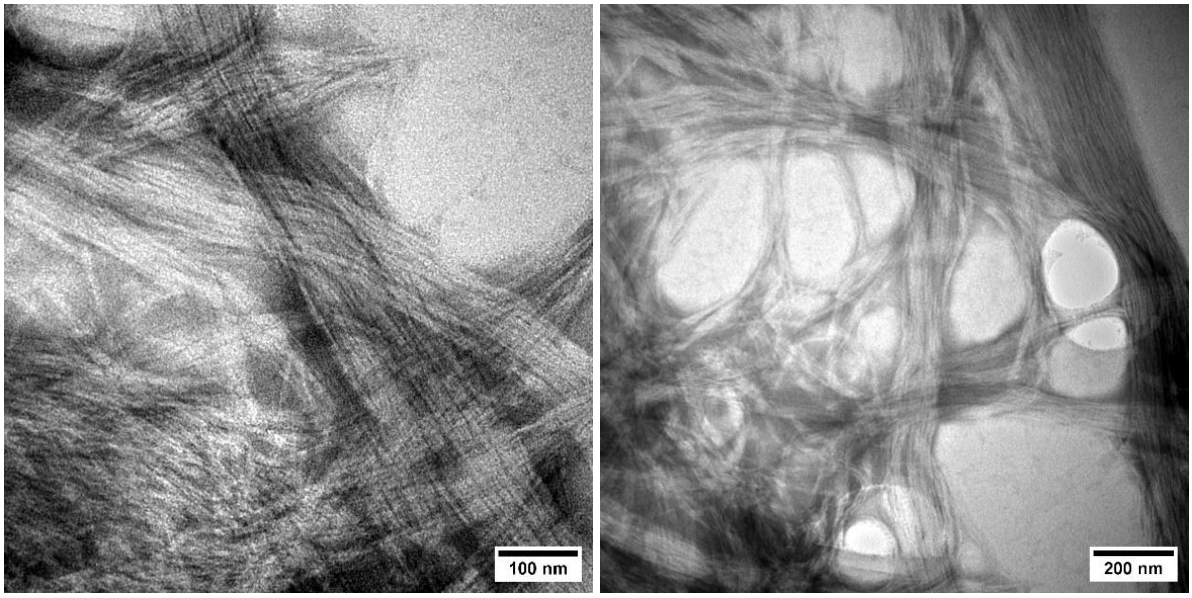

Figure 14: TEM image of CNF with DS = 1.

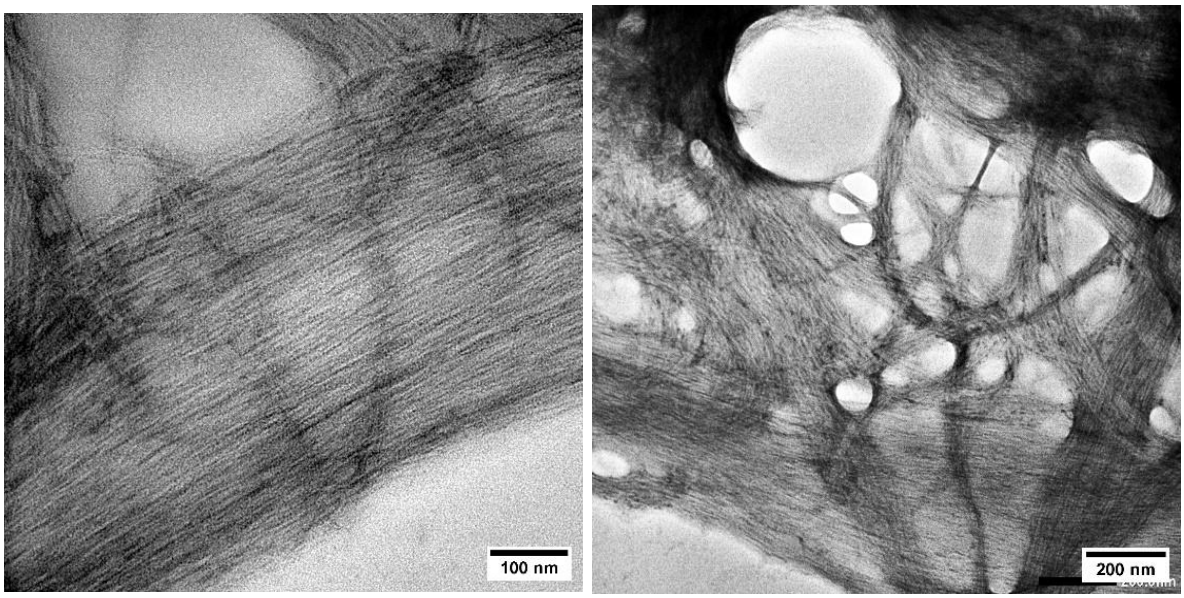

Figure 15: TEM image of CNF with DS = 1.5.

4.1.4 Light microscopy

Light microscopy was done to accompany the TEM images on a macro scale. These images are of air-dried CNF samples and thus agglomeration is expected. Unlike the TEM samples,

these were not treated with a negative stain and the fibres are not as easily seen however due to the much larger scale it is possible to make out the fibre bundles. Figure 16 is of CNF with a DS = 0, the image focuses on a fibre bundle with a diameter of 25 µm. Fibre bundles of this size are common throughout the sample and clearly demonstrate the problem of hornification.

Figure 16: Light microscopy of CNF with DS = 0

Images of the modified CNF show that the acetylation process has had an effect on the material. It is required to edit the images brightness, colour and contrast to make out cellulose fibres in any of the images. This is a good results as the thinner fibres are more difficult to see, these claims are backed by the TEM imaging where the unmodified fibre is tightly held together in a large mass appose to the relatively spread fibres of the modified CNF.

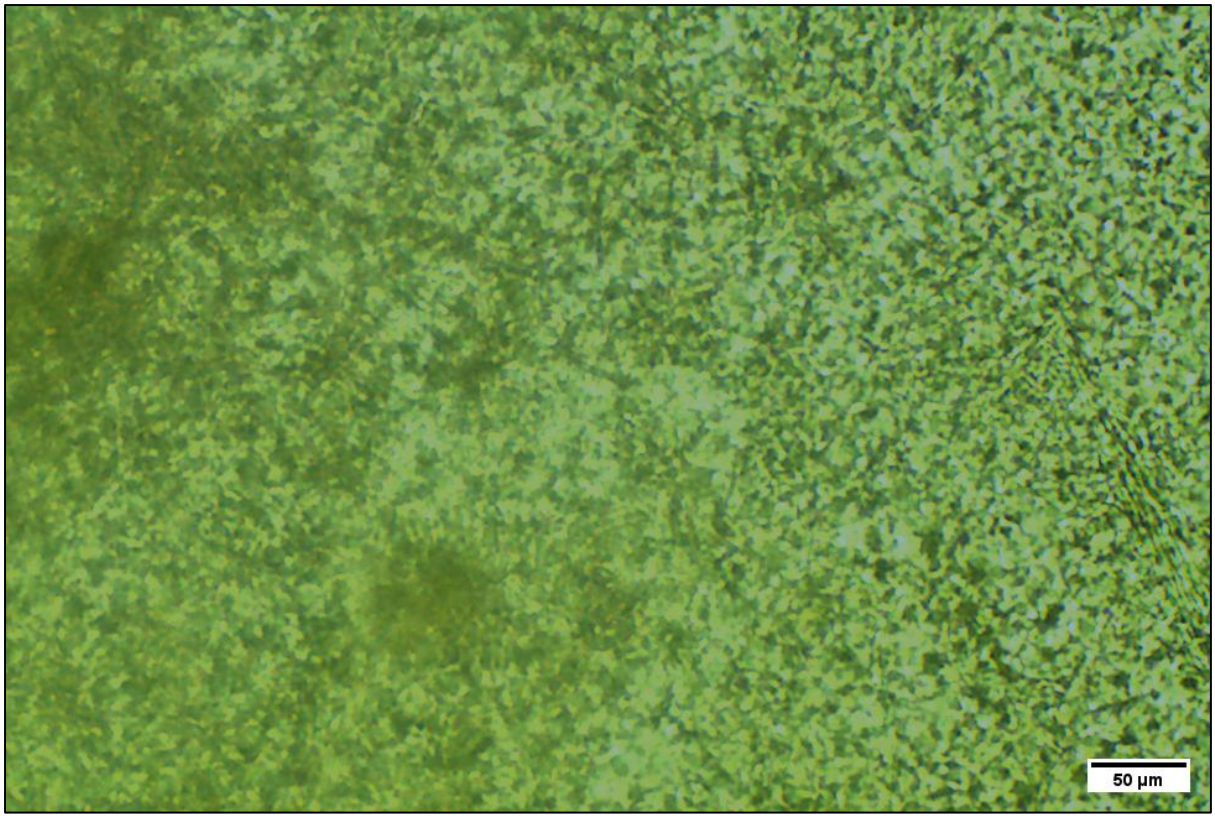

Figure 17: Light microscopy of CNF with DS = 0.5

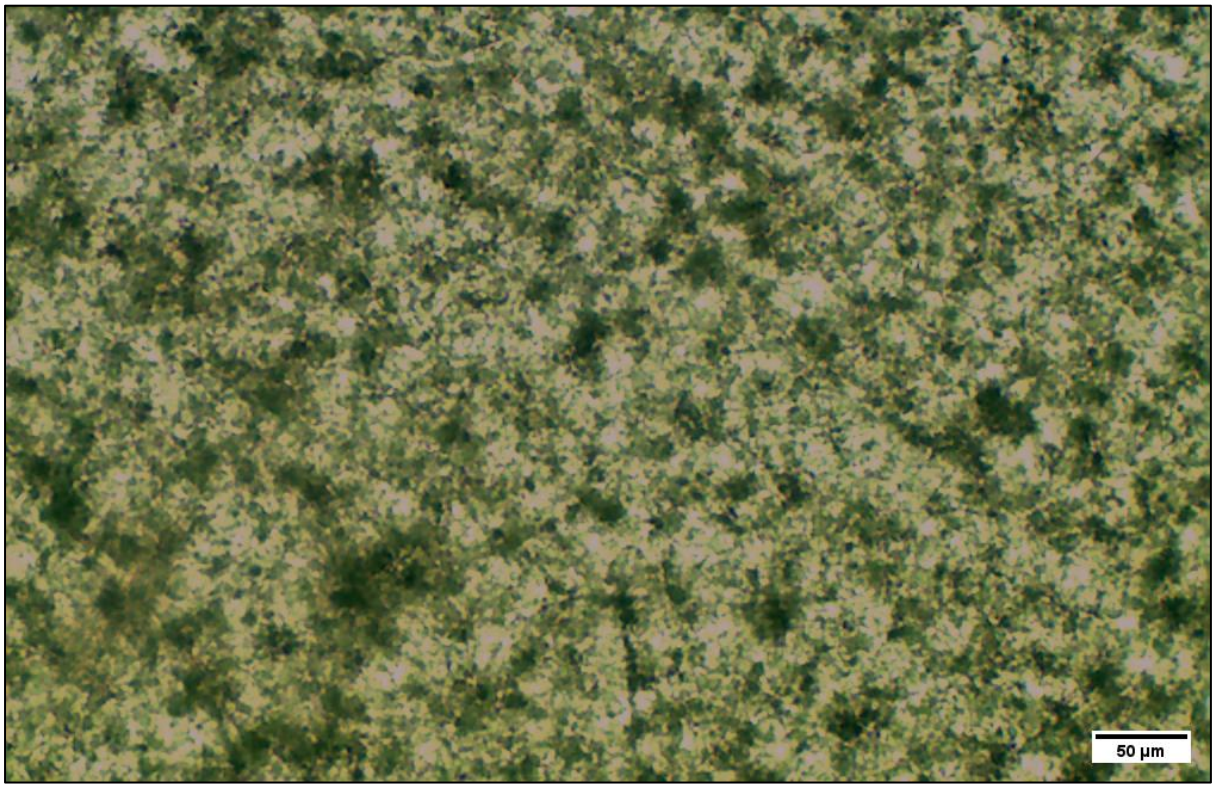

Figure 18: Light microscopy of CNF with DS = 1

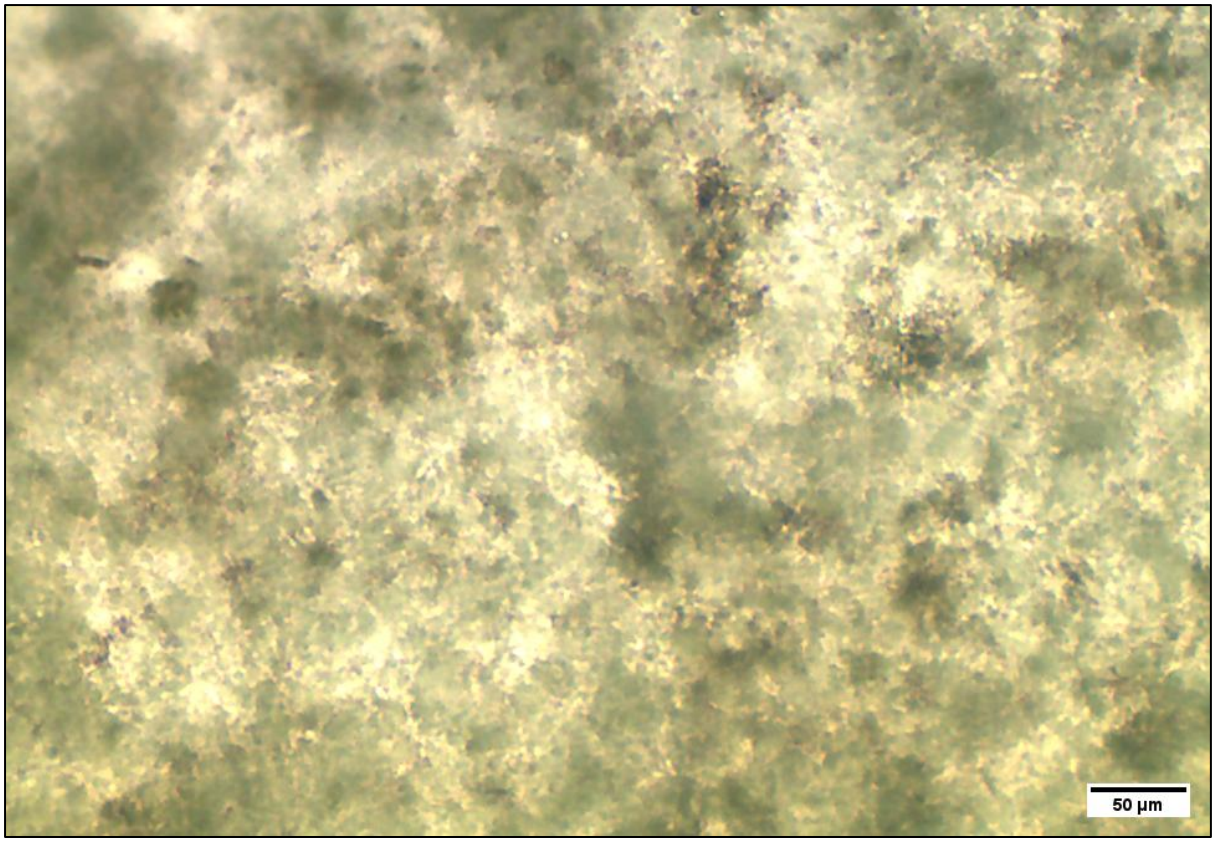

Figure 19: Light microscopy of CNF with DS = 1.5

4.2 Cellulose acetate and cellulose nanofiber composite film

4.2.1 Ultraviolet-visible spectroscopy

Ultraviolet-visible (UV-Vis) spectroscopy can be used to assist the findings of the FTIR due to the fact that CA is a clear plastic while CNF is an opaque fibre that absorbs UV radiation. It is therefore proposed that the more acetylated fibres will absorb less UV radiation. This is in reference to the wavelength at which cellulose absorbs the UV radiation which is taken to be 280 nm. For the 2 % films, the percolation limit was not reached and could be seen through the inconsistency of the films. The other films, namely 5 %, 10 % and 15 %, could be used to show decrease in absorbance with increase in acetylation.

Spectragryph, a software used to analyse UV-Vis data, was used to firstly baseline correct and smooth the spectra before they were rescaled such that the maximum absorbance of all spectra was equal to 1. This peak, at approximately 219 nm, is attenuated to the CA due to the same peak occurring in the Pure film. The other films show a slight shift in this peak however, the information from the 280 nm peak is still viable. The figures below all show the unacetylated CNF has the highest absorbance and a maximum lowering of 35 % of the absorbance with acetylated CNF. The increasing numbers of the graphs represent the increasing DS of the samples, bearing in mind that all graphs in a figure have the same content of CNF it shows that acetylation has taken place. The other common factor is that increasing the DS from 1 to 1.5 will actually increase the absorbance of the films. It is theoreticized that there is essentially a minimum absorbance that can be achieved with the given CNF and as the DS passes a certain limit it will start to disrupt the fibrous network which will cause the absorbance to increase.

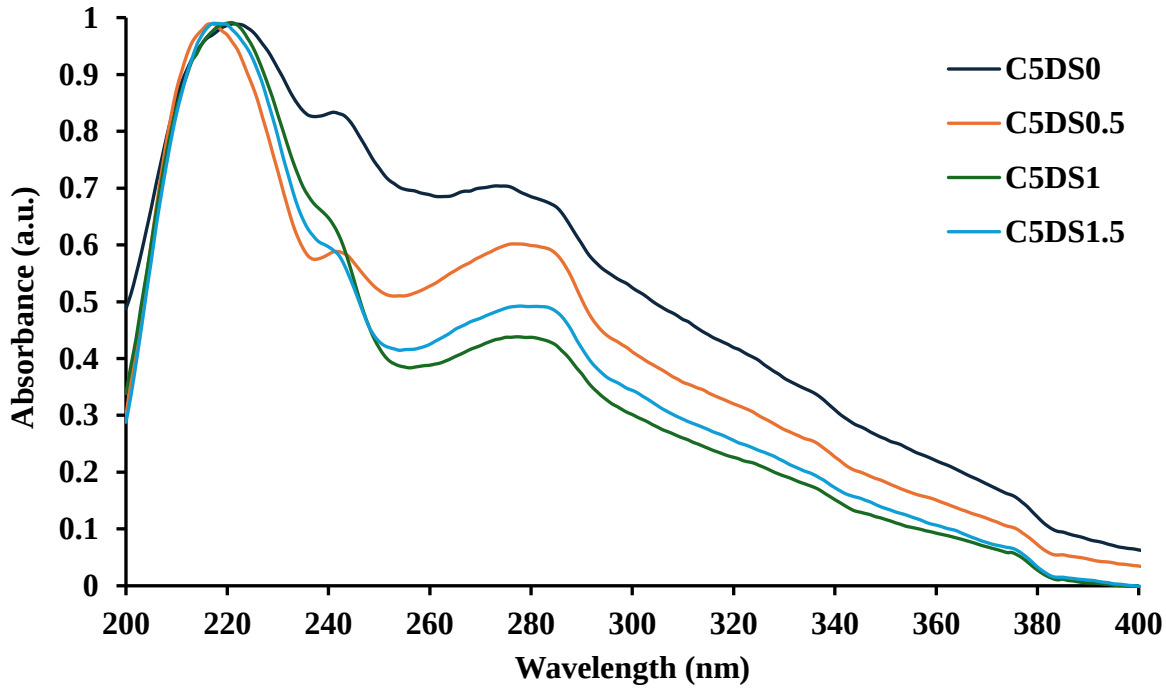

(a) CNF content 5 %

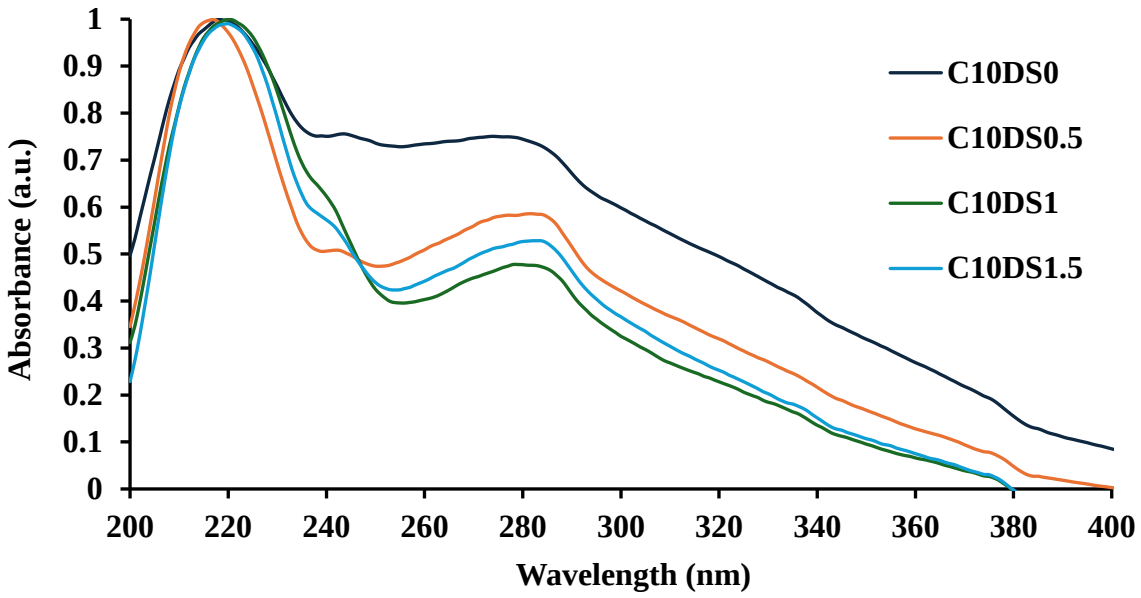

(b) CNF content 10 %

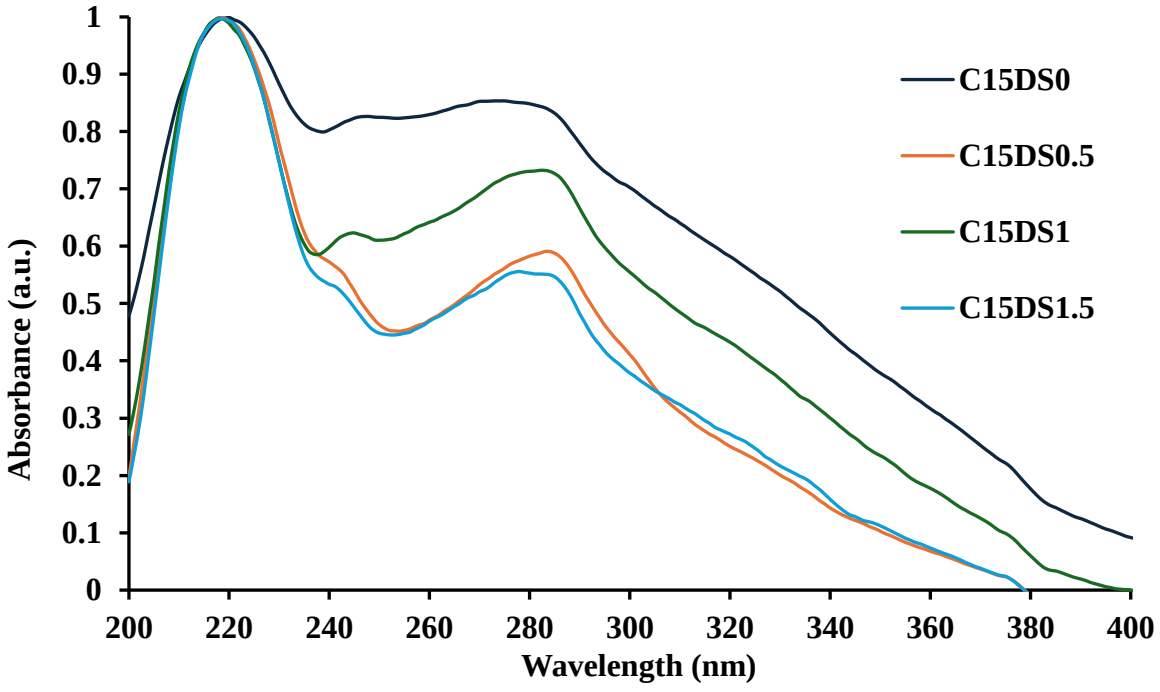

(c) CNF content 15 %

Figure 20: UV-vis spectra of 0.1 mm thick films at different CNF contents.

4.2.2 Water vapour permeability

Table 3 shows the calculated permeabilities of the CA films with increasing CNF content starting at 0 % and going to 15 % with DS kept constant at 1. The calculations were done after the weight of the test samples began to plateau, which took 11 days. The pressure difference was calculated using the vapour pressure of the saturated NaCl salt solution inside the ASTM E96 pots and the vapour pressure inside the desiccator. The trend of the results show that an increase in the CNF content will slightly increase the WVP of the film. This excluded film C2DS1, which at a CNF content of 2 % has a decreased WVP. This is thought to be due to the fact that the percolation threshold was not reached by films with a CNF content of 2 % and thus would not affect the WVP negatively. The remaining films follow the logic that when a dissimilar material, in this case CNF, which has an affinity for water, is introduced into the matrix it will allow more water through the film. This trend does align with other research but due to the different test parameters, such as the salt solution choice, a direct comparison cannot be made (Zhou *et al*, 2021).

Table 3: WVP of films with DS = 1.

Film Number	WVP (10^{-9} gm^{-1} $d^{-1}kPa^{-1}$)
Pure	1.19 ± 0.25
C2DS1	0.51 ± 0.05
C5DS1	1.25 ± 0.23
C10DS1	1.3 ± 0.13
C15DS1	1.36 ± 0.27

4.2.3 Differential scanning calorimetry

The results from the DSC showed that the T_g for all samples is around 100 ºC which is in line with research for CA with this percentage of plasticizer (Phuong *et al*, 2014). A slight increaseing trend in the T_g was observed with an increase in the CNF content, this follows logic as adding a stiff fibre will hinder the ability of a polymer to flow. The decomposition temperature (T_d) of the films could also be determined from the DSC by taking the point at

which the maximum heat flux is absorbed into the sample which would indicate the initial breaking down of the film (Trivedi *et al*, 2015). This value was calculated from the average of two runs, as unlike the T_g results, the T_d had a much larger variance between samples. As a redundancy, TGA analysis was used as a more refined method in determining the decomposition of the film and is discussed further in the paper.

Table 4: T_g and T_d values extracted from DSC curves at a heating rate 0f 10 ºC/min with a 0.5 ºC confidence interval.

Film Number	T_g (ºC)	T_d (ºC)
Pure	97.3	245.4
C2DS1	95.3	254
C5DS1	100	238.8
C10DS1	104	252.2
C15DS1	109.7	210.2

4.2.4 Dynamic mechanical analysis

The main goal of the DMA analysis was to accurately confirm the glass transition temperature of the films. Due to the nature of CA being a relatively tough plastic and the fairly low content of the CNF, the results of the DMA do not show a huge difference in terms of the T_g of the films. This was found through the peaks of the tan delta curves as seen in Figure 21 with exact values displayed in Table 5. Note the confidence interval for this table is high due to the need to smooth the graphs. Film C5DS1 is an outlier which was confirmed through four repeat runs which all produced a similar result. The reason for this much lower T_g is unknown and does not agree with the DSC values. The remainder of the results all exist around the neat CA leading to the conclusion that at a plasticizer loading of 25 %, the addition of CNF up to 15 % does not have an effect on the glass transition temperature of the film.

Table 5: T_g estimated from the peak position of the tan δ curved obtained at a frequency of 1 Hz with a confidence interval of 2.5 ºC.

Film Number	T_g (ºC)
Pure	91.5
C2DS1	92.4

C5DS1	77.2
C10DS1	88.1
C15DS1	90.1

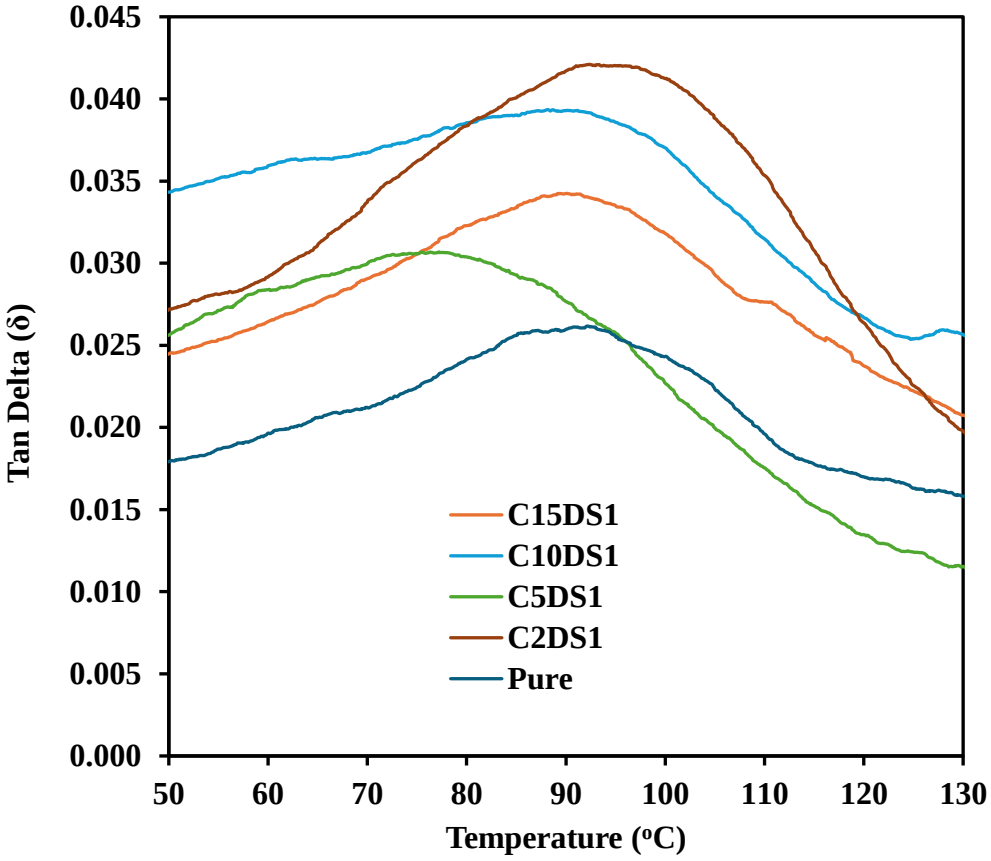

Figure 21: Tan Delta curves of films.

4.2.5 Thermogravimetric analysis

CA has a standard thermal decomposition temperature just above 370 °C. However, the addition of CNF essentially breaks this decomposition into two parts. The effect of the CNF on thermal stability is shown in the TGA analysis of the figures below. The results show that there seems to be an antagonistic relationship since the higher the CNF content in the film, the lower the temperature it will begin to decay at. This temperature is lower than the pure CNF sample, which is analysed without a plasticizer which explains why its decay temperature is high, but

it is unknown to what degree this effect is. The derivative weight graph is also a great indication of the CNF content and essentially shows how the breakdown of the film is split into two different temperature regions, the first at 250 ºC and the second at 370 ºC. These results do raise a concern to the viability of the use CNF in CA however, plasticized CA is rarely used above the glass transition temperature which is far below the first decomposition (Moelter and Schweizer, 1949).

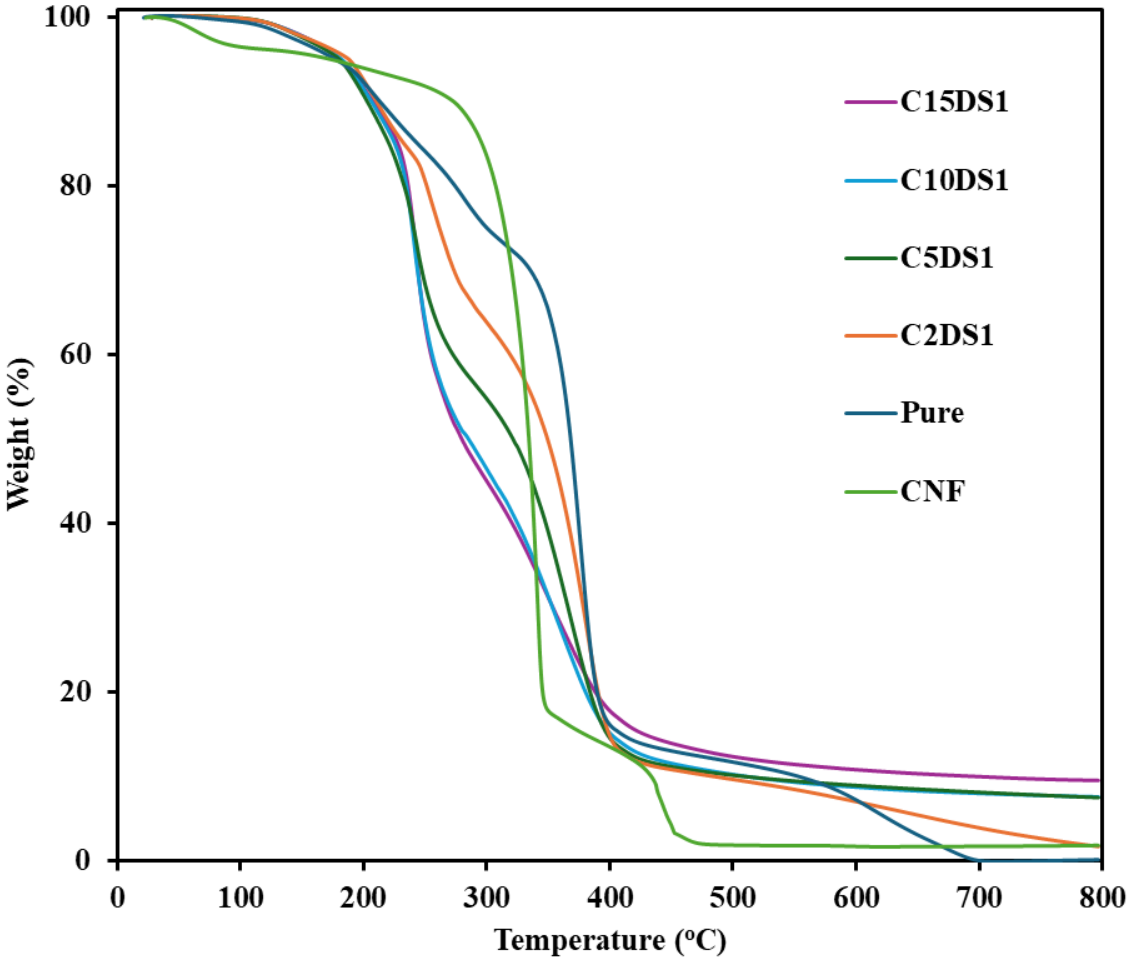

Figure 22: Mass Change of Samples.

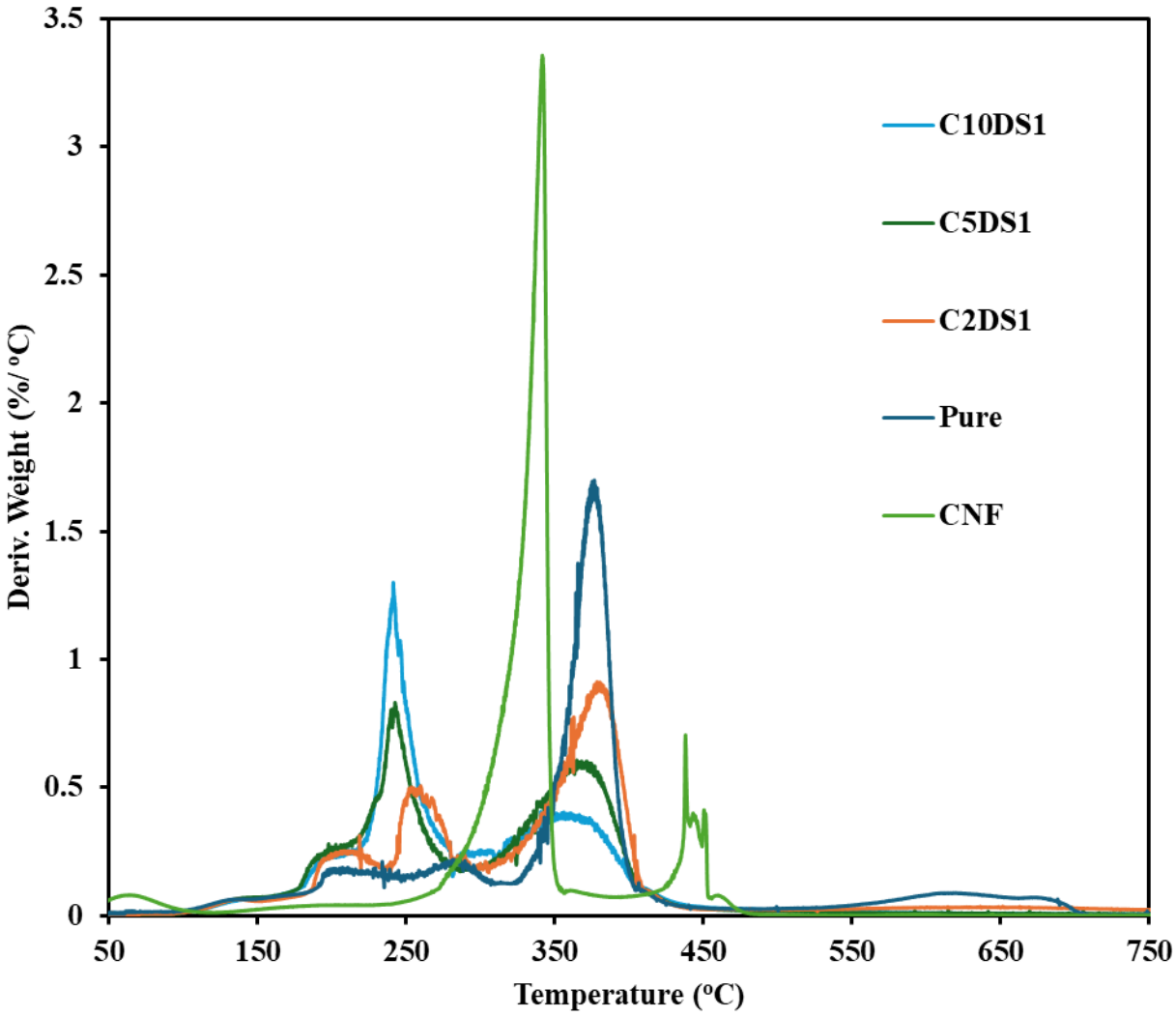

Figure 23: Derivative of mass change.

4.2.6 X-ray diffraction

Similarly to the derivative of mass change graph from the TGA, the XRD analysis of the CA/CNF films shows that two reflections of crystallinity will form. The first isolated peak, at 8°, relates to the Van der Waals halo which also accounts for the rise around 22°. These peaks indicate the crystalline CA with an interplanar distance of 11.1 Å (Rodrigues Filho *et al*, 2000). As the same in the characterisation of the acetylated CNF, the peak at 28° is attenuated to type I_β cellulose. The graph mainly shows the ratio change between these two crystallinities as the

CNF content increases however film C15DS1 shows a high and sharp reflections at both points of interest, leading to the conclusion that it is more crystiline. Film C5DS1 is a shortcoming as its reflection for CA is far below the expected height, the reason for this is unknown. The results are useful to show that the highly crystalline CNFs will exponentially increase the crystallinity of the matrix with an increase in the CNF content.

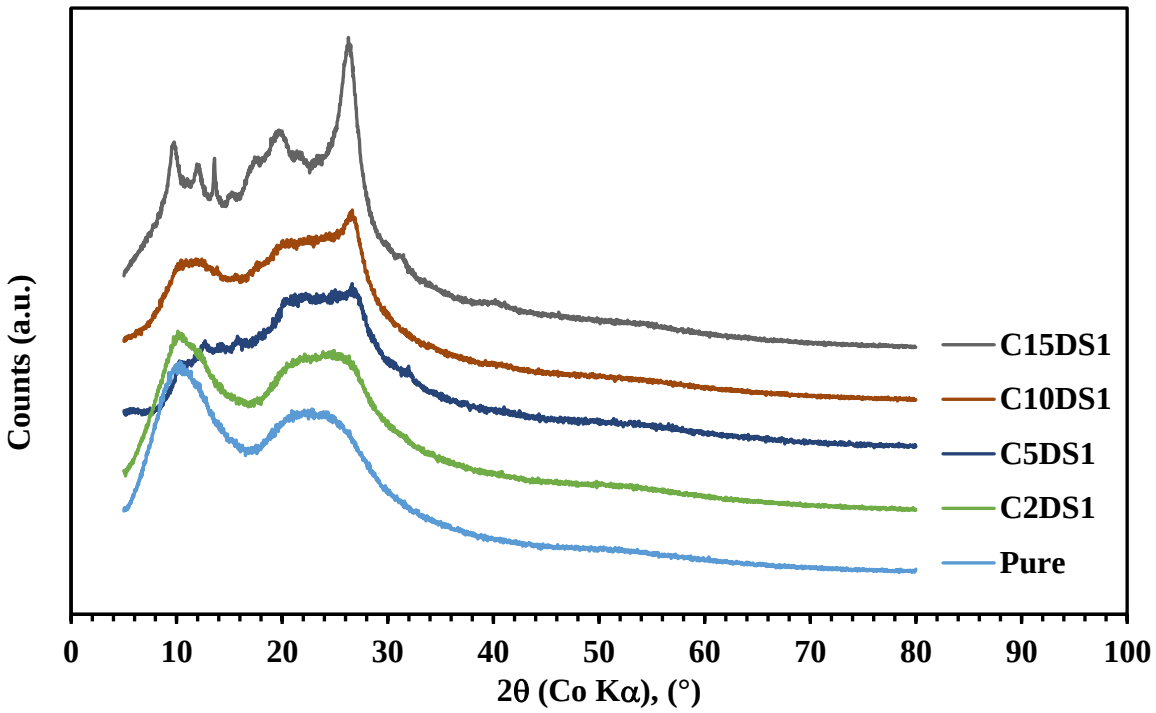

Figure 24: XRD analysis of films.

4.2.7 Scanning electron microscopy

SEM imaging did not produce any noteworthy micrographs. There are two proposed reasons for this. First is due to the similarity between the CA and CNF chains, the imaging was not able to show the presence of the nanofibers. This is backed by the need of negative staining for the TEM imaging to simply show the fibres themselves. The second reason is believed to be an error in making the films which resulted in the section of film being analysed not containing any CNF. To combat these poor findings, light microscopy was used to analyse the CNF in CA.

4.2.8 Light microscopy

The scale used for the light microscopy was able to clearly show the effect acetylation had on fibre diameter. This allows a decisive measurement to confirm that the methodology has played an effect on the agglomeration of the CNF. Figure 25 is an image of 15 % unmodified CNF, DS = 0, in CA and shows that the highly process nanofibers, which initially start with a diameter of 100 nm, collapse together and form fibres that can reach up to 25 µm in diameter. The hydrogen bonding which forms between the fibres is too strong a force and the irreversible hornification process takes place. Figure 26, which also shows a film with 15 % CNF, contains fibres that have been acetylated to a DS of 1.5. This is the highest acetylation used in this research but shows the shear difference to the unacetylated CNF. This image shows that there are still fibers present with lengths well over 100 µm however, the diameter of these fibers do not exceed 5 µm. This is a 5-fold improvement and essentially says that for the same amount of CNF in both samples, there are five times as many individual fibres in the acetylated sample. At this relatively high DS there is also the chance that nanocrystals will form as a byproduct. These nanocrystals are difficult to find but Figure shows what they look like in the CA film. Due to the scarcity of these CNCs, they do not pose a problem to the results.

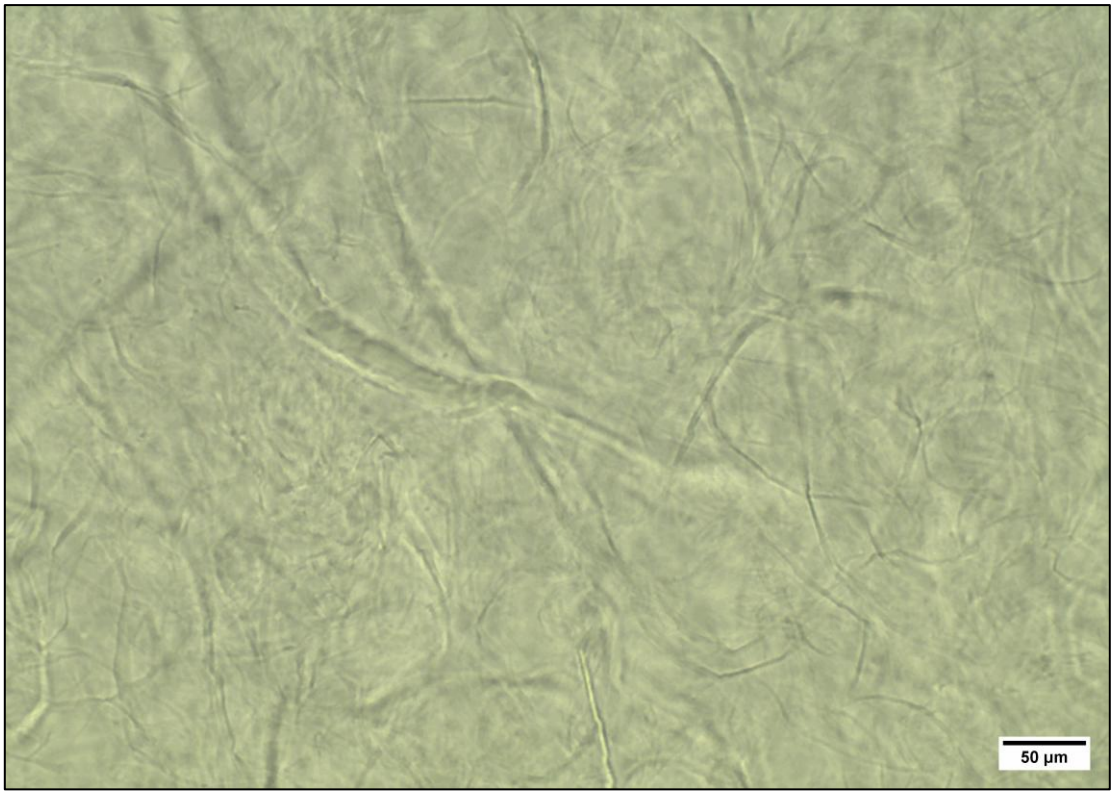

Figure 25: Light microscopy image of film C15DS0.

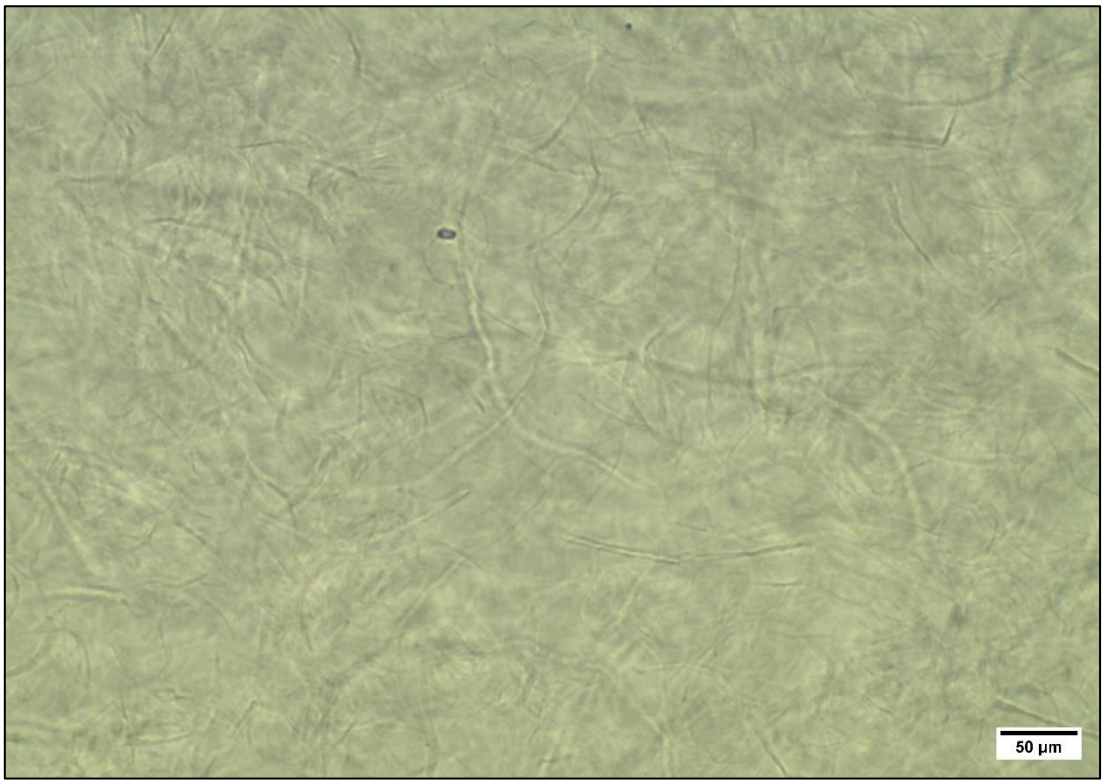

Figure 26: Light microscopy image of film C15DS1.5.

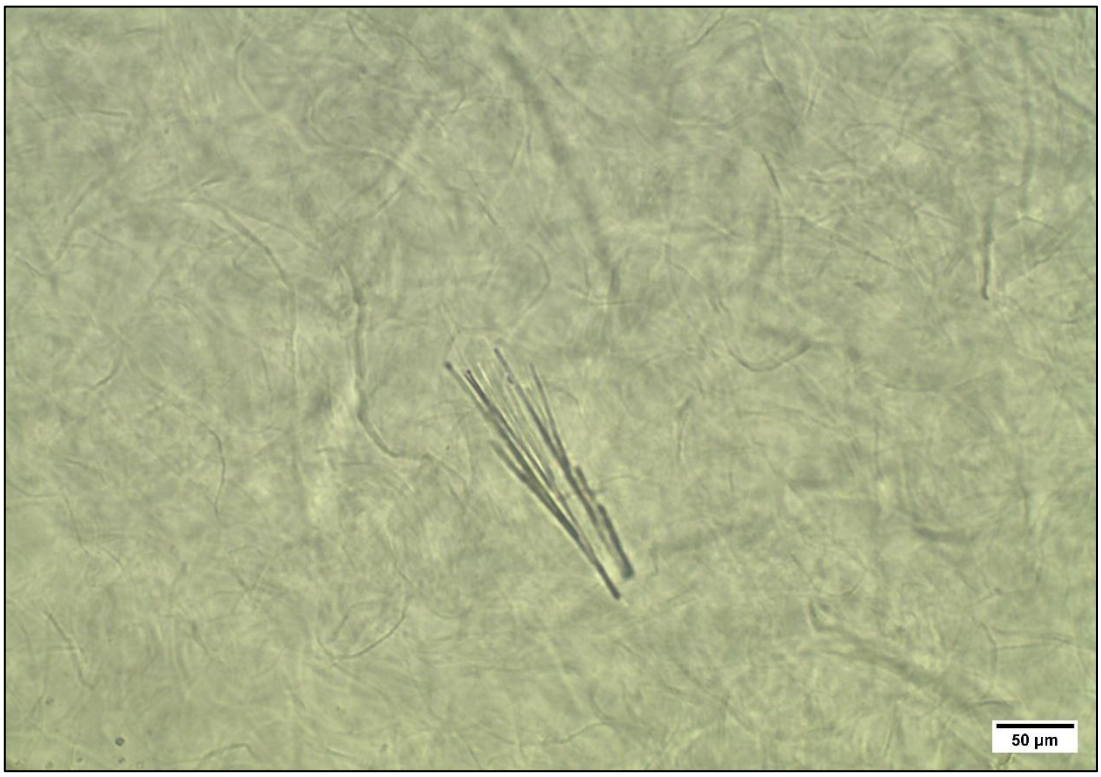

Figure 27: Light microscopy image of CNCs from film C15DS1.5.

4.2.9 Mechanical testing

All the measured values shown a CA plastic that has lower values than what is potential, however the importance lies in the comparison between the tested samples and not with other research(Charvet *et al*, 2019). potential Figure 28 displays the stress-strain curves for neat CA and all the films that have a DS = 1. These films showed the best trend and were thus used for this graph. First, one can notice the increased gradient from the neat CA which follows the logic of nanofibres increasing the stiffness. There is also a slight increase in the maximum tensile stress with an increase with acetylation which could be due to the increased dispersion of the fibres. The main point of interest however is the yield point of the films. The pure film and film C10DS0 are comparatively ductile and yield at low strengths which in certain cases is desirable but show that strength is being lost to when the plastic yields. In other words, the addition of the CNF does not have an effect. The acetylated CNF films, however, show that

instead of yielding at a lower point all the strength is used before the yield point. This allows the plastic to absorb more energy before plastic deformation occurs.

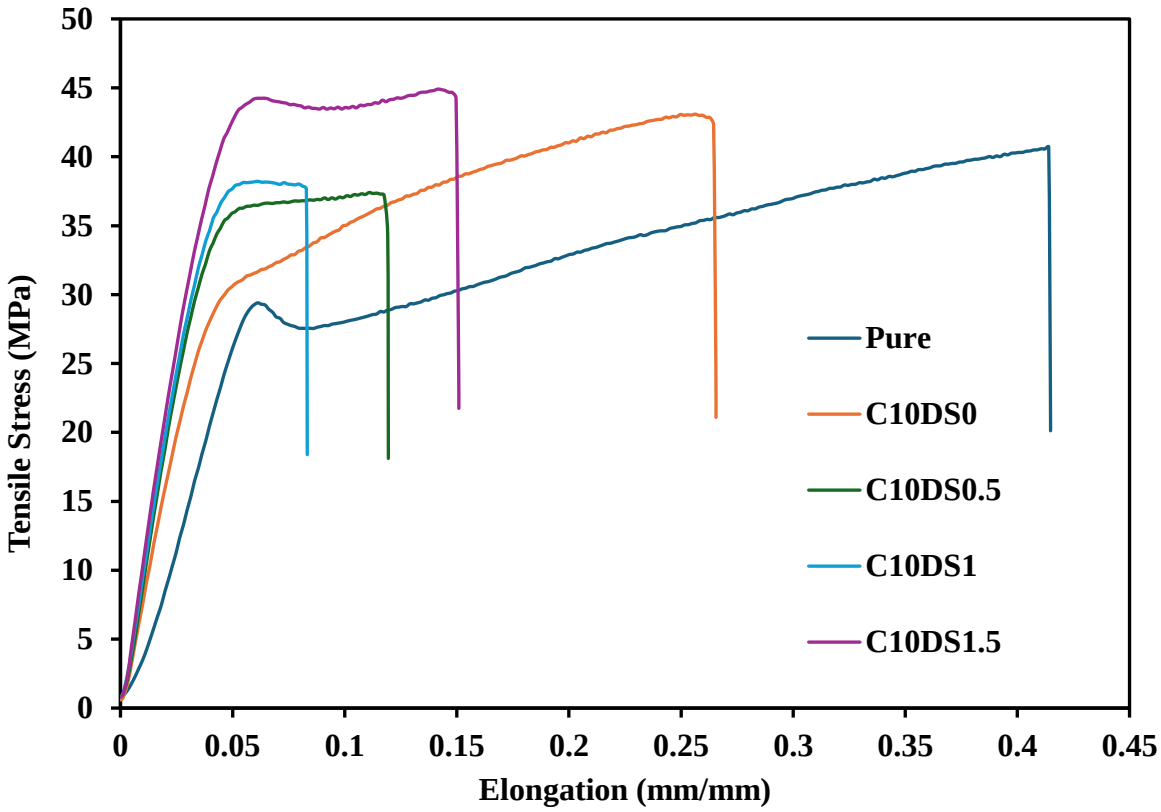

Figure 28: Effects of added acetylated CNF on the tensile properties of cellulose acetate films.

The Youngs modulus, or modulus of elasticity, is the ratio of tensile stress to tensile strain and tells us how a material will deform when a force is applied to it. The graph for all the films tested is shown in Appendix B and table 6 displays the values for the respective bar graphs, note the Pure film with 0 % CNF is used as a reference across all samples. Results are grouped into films with the same CNF content with each group increasing the DS from left to right, this is the same for the tensile strength graph. The best results from the 10 % CNF group show that by simply acetylating the fibres to a DS of 0.5, there is a 250 % strength increase compared to the unacetylated sample. The consistency of the graphs is not ideal but only in two films out of the sixteen test films does it show that the acetylation of the nanofibres harms the films properties. There is also some variation within the acetylated samples such as film C15DS1.5 which produces a value far below what is expected. The other graphs show an improvement of

some degree and generally show that the improved dispersion aids in the films ability to absorb more energy before breaking.

Table 6: Modulus of elasticity of films (MPa).

CNF Content (%)	Degree of Substitution 0	0.5	1	1.5
0		707 ± 41		
2	987 ± 83	987 ± 83	987 ± 83	987 ± 83
5	1007 ± 102	1007 ± 102	1007 ± 102	1007 ± 102
10	789 ± 76	789 ± 76	789 ± 76	789 ± 76
15	952 ± 128	952 ± 128	952 ± 128	952 ± 128

To get a better understanding of the Youngs modulus, the Halpin-Tsai equation is used to link the CNF volume fraction to the expected modulus. A modified equation is used as below (Tucker III and Liang, 1999).

$$\frac{E_c}{E_m} = \frac{1+cv_f}{1-\eta v_f} \quad \text{with} \quad \eta = \frac{(\alpha E_f/E_m)-1}{(\alpha E_f/E_m)+c} \tag{1}$$

E_c refers to the modulus of the composite polymer while E_m and E_f refer to the modulus of the neat polymer and fibre reinforcement respectively, v_f is the volume fraction of the fibre, c is the shape factor of the fibre and α pertains to the orientation factor. The shape factor is further described as

$$c = \frac{2l}{d} e^{-av_f - b} \tag{2}$$

where l and d are the fibre bundles length and diameter while a and b are constants which account for the agglomeration of the CNF (Sun *et al*, 2011). The orientation factor is taken as a third due to the random orientation and fibre aspect ratio as explained in (Cox, 1952). The modulus from the neat sample above is used while the modulus for pure CNF is taken as 115 GPa (Zhai *et al*, 2018). Fitting the data points from the DS = 0 and DS = 1 samples to the theoretical curve, with $a = 8$ and $b = 0.5$, it can be seen how much better the acetylated sample fits the curve which reinforces the claim that the acetylation has improved the dispersion. There is still a drop off at higher CNF content values presumed to be from large agglomeration bundles acting as stress concentrations in the film (Sun *et al*, 2011).

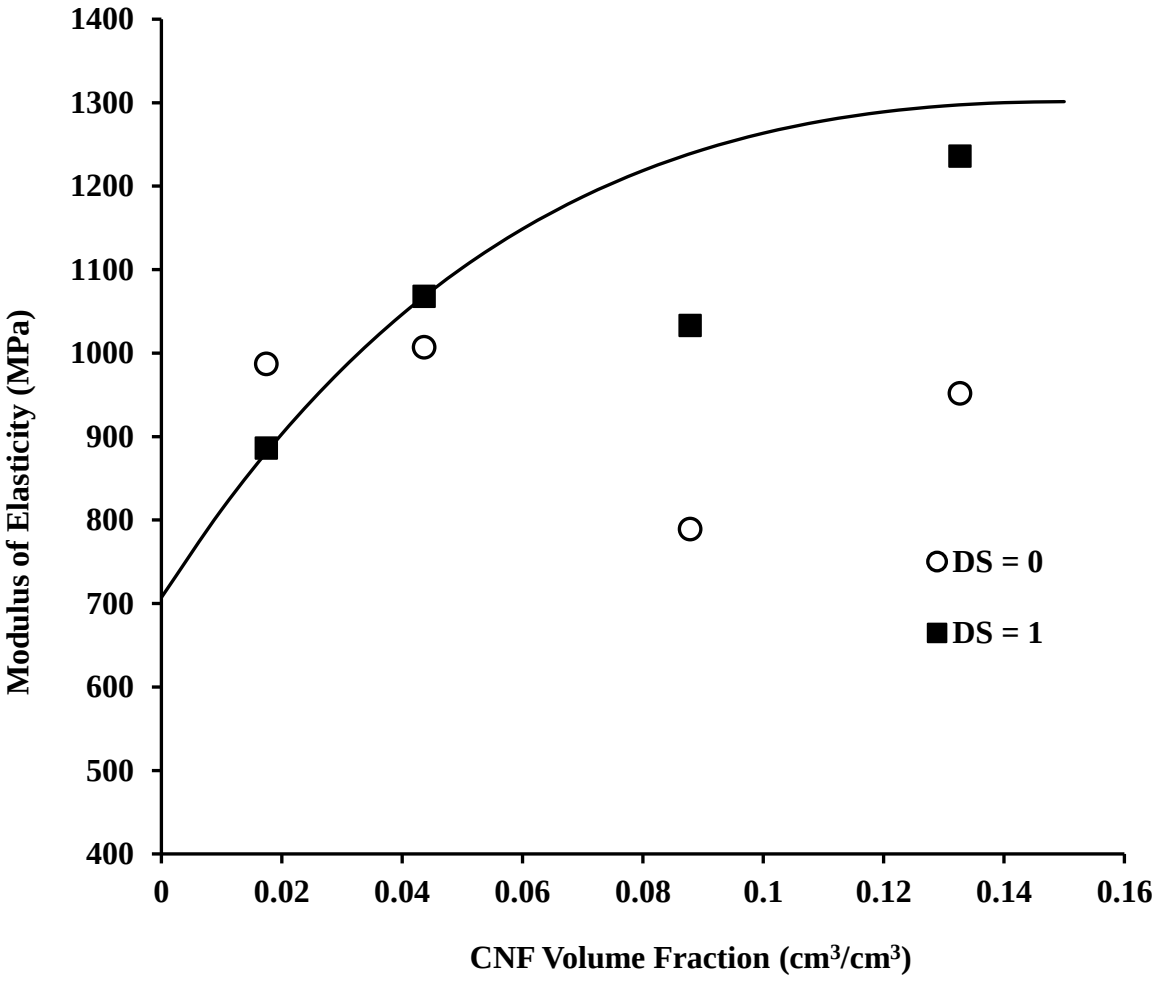

Figure 29: Experimental Youngs modulus and theoretical fit from Halpin-Tsai equation.

The tensile stress graph, Figure 31 and respective table Appendix C, does not display any effect from the acetylation of the CNF. This is attributed to the similar strengths between CA and CNF. Unlike the modulus of elasticity, the tensile strength graph simply shows the force at which the film will break. As can been seen from the graph, CA is already a strong polymer, and the acetylation of CNF will not change the maximum amount of force the polymer will take before it breaks. At the tested sample thickness, there is not enough conclusive evidence to determine the effect of acetylation.

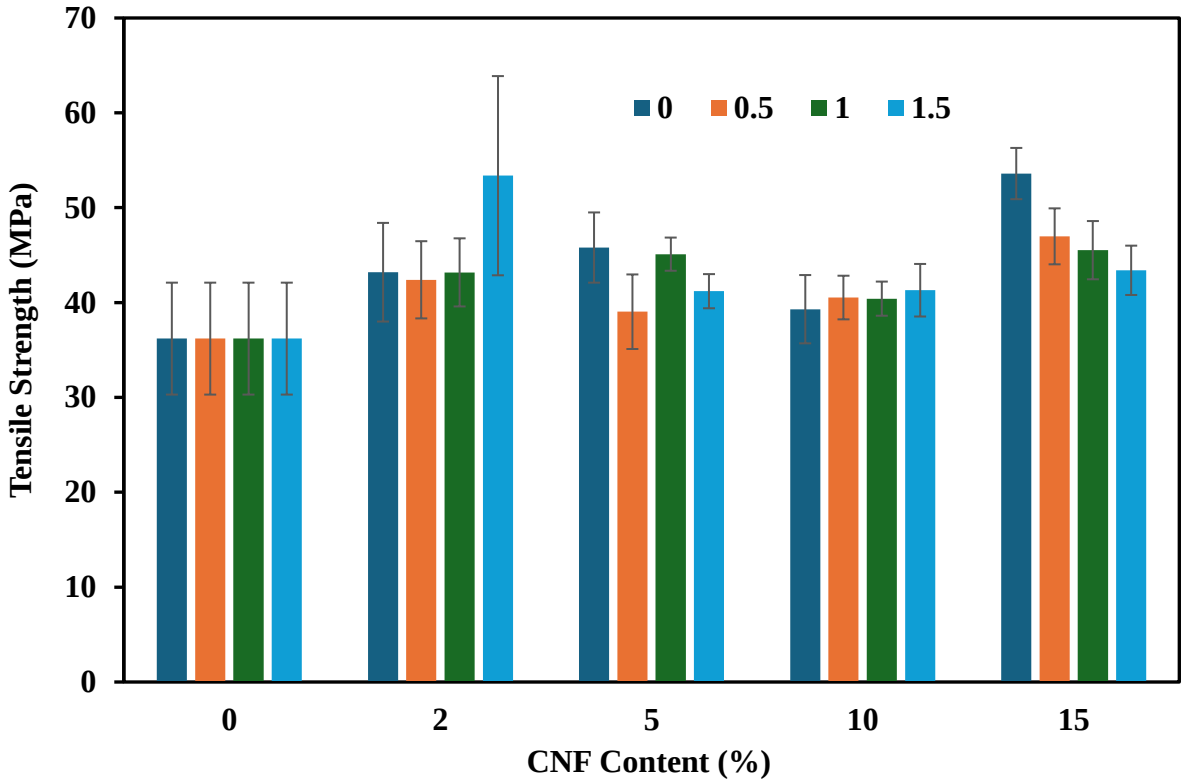

Figure 30: Tensile strength of films.

4.3 Discussion

In terms of the effect of the acetylation on the pure CNFs, it can be concluded that no damage was done to lengths of the fibers even though acetylation had occurred. The DS has been accurately controlled, which is confirmed by the FTIR, demonstrating that the azeotropic distillation and treatment of the CNFs can lead to a water free paste. The necessity to perform a complete solvent swap with acetic acid is a vital process and is shown to be successful. XRD and microscopy imaging show that the degree of crystallinity remains unchanged in the wet paste however the dried nanocellulose paper has fibre bundles with a much smaller diameter as well as a higher degree of dispersion within the throughout the material.

The use of high shear mixing in the preparation method is of vital importance to the final product. Initial testing demonstrated that without the use of the Silverson L4RT there would be large inconsistencies within the films. With regard to the methodology as a whole, the ability to produce a quality film via solvent casting is an inexpensive and convenient production method. This, however, does not limit the production method but further research would need to be done in order to determine the effect in extrusion, injection moulding and other production methods. It is predicted that the results will align with the outcomes of this report but there is the possibility of the increased temperatures in the above-mentioned processes negatively affecting the final product.

The incorporation of CNFs into CA with fibre diameters as small as 5 nm led to a number of issues yet there was success in improving the quality of the film. Agglomeration is the enemy of CNFs and throughout testing can be seen to have an effect in the unmodified sample. It is confirmed in imaging that there is a high degree of hornification resulting in large fibre bundles. Compared to the modified samples there is a clear difference in the fibre diameter which can also be deduced from UV-Vis as samples with the same CNF concentration will become more transparent with acetylation. This difference is small however when scaled up can lead to major differences in the cost of material.

Compared to other bioplastic composites with CNF, such as TPS and PLA, CA does not perform as well. As shown this is due to the chemical structure of cellulose acetate not being able to bond naturally with CNF like PLA. The ability to not only reduce the fibre bundle diameter but also with the added benefit of improved dispersion into the matrix is a big step to

a high performing biodegradable polymer. Also, the reduced fibre diameter means that for the same cost of material there will be a greater number of cellulose fibres, as much as five times, and better dispersed throughout the matrix. This does not directly translate to the mechanical properties of the films, but the trend shows that any degree of acetylation will improve the quality of the film.

5 Conclusion

The ability to make improved biodegradable polymer composites is an ever-growing topic and with the above research can lead to impressive findings. Lately, there has been a rise in research of cellulose nanofibres being used as a strengthening agent in polymer composites such as in polylactic acid. It has been shown that cellulose acetate can also benefit from cellulose nanofibres through the partial acetylation of the fibre. Acetylation, through the use of acetic anhydride, can improve the dispersion of cellulose nanofibres in a polymer blend but is a fairly complex and costly process to achieve the correct degree of substitution. This method has been proven to work and has been confirmed through Fourier transform infrared analysis. A degree of substitution as low as 0.5 can have huge effects on the postproduction diameter of fibers, optical transparency and toughness. Higher acetylation's can yield improved results but come at the risk of damaging the fibre and creating cellulose nanocrystals. Through this process the cellulose nanofibres retains its high shear thinning property opening the door for potential applications in the solvent casting method where a certain shape can be set without the need for a mould. This research is also not limited to the solvent cast method but is also just as viable in other processing methods such as screw extrusion and injection moulding.

Imaging of both the plain cellulose nanofibres samples and the cellulose acetate composites showed that acetylation of the surface hydroxyl groups does lead to improved dispersion of the fibers. Fibre diameter in unmodified samples can be five times greater than that of acetylated samples. This means that for the same amount of cellulose nanofibres in both samples, there are five times as many individual fibers in the acetylated sample. This could lead to improved properties if the cellulose acetate polymer were to redissolve into a solution. Further research needs to be done in this aspect. Research into the acetylation of dried cellulose nanofibres with xanthan is also needed.

Tensile testing of the films revealed that the potential for further improvement of cellulose acetate from cellulose nanofibres is possible and can lead to a biodegradable material that is simple to make but with a high level of toughness comparable to the competitive market. The best results, at a cellulose nanofibres content of 10 % and a degree of substitution of 0.5, showed that the acetylation of cellulose nanofibres can more than double the effect on the Youngs modulus of the cellulose nanofibres in the film. The films with higher acetylations did not display any major benefits and it is recommended that they be avoided due to the creation of cellulose nanocrystals. This research is not limited to cellulose acetate as the matrix. Similar polymers with strong electrostatic groups, like the double bonded oxygen, should respond in the same way to the acetylated cellulose nanofibres. Examples of these plastics include PBS and other polyhydroxyalkanoates.

6 References

Abu-Zurayk, R, Alnairat, N, Khalaf, A, Ibrahim, AA, and Halaweh, G (2023), "Cellulose acetate membranes: Fouling types and antifouling strategies—A brief review" *Processes*, 11(2), 489.

Ach, A (1993), "Biodegradable Plastics Based on Cellulose Acetate" *Journal of Macromolecular Science, Part A*, 30(9-10), 733-740.

Agate, S, Joyce, M, Lucia, L, and Pal, L (2018), "Cellulose and nanocellulose-based flexible-hybrid printed electronics and conductive composites–A review" *Carbohydrate Polymers*, 198249-260.

Allen, JC, and Barnes, DF (1985), "The causes of deforestation in developing countries" *Annals of the association of American Geographers*, 75(2), 163-184.

Arbelaiz, A, Ibarbia, J, Imaz, B, and Soto, L (2023), "Natural Fiber–Reinforced Cement Mortar Composite Physicomechanical Properties: From Cellulose Microfibers to Nanocellulose" *Journal of Materials in Civil Engineering*, 35(5), 04023094.

Ashori, A, Babaee, M, Jonoobi, M, and Hamzeh, Y (2014), "Solvent-free acetylation of cellulose nanofibers for improving compatibility and dispersion" *Carbohydrate Polymers*, 102369-375.

Aspinall, GO (2014), The polysaccharides, Academic Press,

Aulin, C, Gällstedt, M, and Lindström, T (2010), "Oxygen and oil barrier properties of microfibrillated cellulose films and coatings" *Cellulose*, 17559-574.

Azimi, B, Maleki, H, Gigante, V, Bagherzadeh, R, Mezzetta, A, Milazzo, M, Guazzelli, L, Cinelli, P, Lazzeri, A, and Danti, S (2022), "Cellulose-based fiber spinning processes using ionic liquids" *Cellulose*, 29(6), 3079-3129.

Badgujar, KC, Dange, R, and Bhanage, BM (2021), "Recent advances of use of the supercritical carbon dioxide for the biomass pre-treatment and extraction: A mini-review" *Journal of the Indian Chemical Society*, 98(1), 100018.

Ballesteros, I, Duque, A, Negro, M, Coll, C, Latorre-Sánchez, M, Hereza, J, and Iglesias, R (2022), "Valorisation of cellulosic rejections from wastewater treatment plants through sugar production" *Journal of Environmental Management*, 312114931.

Barbu, MC (2011), "Current developments in the forestry and wood industry" *Pro Ligno*, 7(4).

Berto, GL, and Arantes, V (2019), "Kinetic changes in cellulose properties during defibrillation into microfibrillated cellulose and cellulose nanofibrils by ultra-refining" *International Journal of Biological Macromolecules*, 127637-648.

Bertram, R, Pedersen, MG, Luciani, DS, and Sherman, A (2006), "A simplified model for mitochondrial ATP production" *Journal of theoretical biology*, 243(4), 575-586.

Blok, AE, Bolhuis, DP, Kibbelaar, HVM, Bonn, D, Velikov, KP, and Stieger, M (2021), "Comparing rheological, tribological and sensory properties of microfibrillated cellulose dispersions and xanthan gum solutions" *Food Hydrocolloids*, 121107052.

Braun, D, Cherdron, H, and Ritter, H (2001), Polymer synthesis: theory and practice: fundamentals, methods, experiments, Springer,

Carvalho, DMd, Berglund, J, Marchand, C, Lindström, ME, Vilaplana, F, and Sevastyanova, O (2019), "Improving the thermal stability of different types of xylan by acetylation" *Carbohydrate Polymers*, 220132-140.

Cazón Díaz, P, Morales Sánchez, E, Velázquez, G, and Vázquez Vázquez, M (2022), "Measurement of the water vapor permeability of chitosan films: a laboratory experiment on food packaging materials".

Chaabouni, O, and Boufi, S (2017), "Cellulose nanofibrils/polyvinyl acetate nanocomposite adhesives with improved mechanical properties" *Carbohydrate Polymers*, 15664-70.

Charvet, A, Vergelati, C, and Long, DR (2019), "Mechanical and ultimate properties of injection molded cellulose acetate/plasticizer materials" *Carbohydrate Polymers*, 204182-189.

Cheng, G, Zhou, M, Wei, YJ, Cheng, F, and Zhu, PX (2019), "Comparison of mechanical reinforcement effects of cellulose nanocrystal, cellulose nanofiber, and microfibrillated cellulose in starch composites" *Polymer Composites*, 40(S1), E365-E372.

Cheng, M, Qin, Z, Hu, J, Liu, Q, Wei, T, Li, W, Ling, Y, and Liu, B (2021), "Facile one–step preparation of acetylated cellulose nanocrystals and their reinforcing function in cellulose acetate film with improved interfacial compatibility" *Cellulose*, 28(4), 2137-2148.

Chien, IL, Zeng, K-L, Chao, H-Y, and Liu, JH (2004), "Design and control of acetic acid dehydration system via heterogeneous azeotropic distillation" *Chemical engineering science*, 59(21), 4547-4567.

Chinga-Carrasco, G (2011), "Cellulose fibres, nanofibrils and microfibrils: The morphological sequence of MFC components from a plant physiology and fibre technology point of view" *Nanoscale research letters*, 61-7.

Chu, Y, Sun, Y, Wu, W, and Xiao, H (2020), "Dispersion Properties of Nanocellulose: A Review" *Carbohydrate Polymers*, 250116892.

Cindradewi, AW, Bandi, R, Park, C-W, Park, J-S, Lee, E-A, Kim, J-K, Kwon, G-J, Han, S-Y, and Lee, S-H (2021), "Preparation and characterization of cellulose acetate film reinforced with cellulose nanofibril" *Polymers*, 13(17), 2990.

Cook, SL (1993), "Acetic Anhydride" *Acetic acid and its derivatives*.

Correia, J, Rainert, KT, Oliveira, FR, de Cássia Siqueira Curto Valle, R, and Valle, JAB (2020), "Cationization of cotton fiber: An integrated view of cationic agents, processes variables, properties, market and future prospects" *Cellulose*, 278527-8550.

Cox, HL (1952), "The elasticity and strength of paper and other fibrous materials" *British journal of applied physics*, 3(3), 72.

Cross, C, Bevan, E, and Beadle, C (1895), "XLVII.—Contributions to the chemistry of cellulose" *Journal of the Chemical Society, Transactions*, 67433-451.

Deanin, RD (1987), "History of plasticizers" *History of Polymeric Composites*, 167.

Decroix, C, Chalamet, Y, Sudre, G, and Caroll, V (2020), "Thermo-mechanical properties and blend behaviour of cellulose acetate/lactates and acid systems: Natural-based plasticizers" *Carbohydrate Polymers*, 237116072.

Dizge, N, Shaulsky, E, and Karanikola, V (2019), "Electrospun cellulose nanofibers for superhydrophobic and oleophobic membranes" *Journal of Membrane Science*, 590117271.

Dufresne, A (2019), "Nanocellulose Processing Properties and Potential Applications" *Current Forestry Reports*, 5(2), 76-89.

Eales, J, Bethel, A, Galloway, T, Hopkinson, P, Morrissey, K, Short, RE, and Garside, R (2022), "Human health impacts of exposure to phthalate plasticizers: An overview of reviews" *Environment international*, 158106903.

El-Wakil, N, Taha, M, Abouzeid, R, and Dufresne, A (2022), "Dissolution and regeneration of cellulose from N-methylmorpholine N-oxide and fabrication of nanofibrillated cellulose" *Biomass Conversion and Biorefinery*, 1-12.

Endo, R, Setoyama, M, Yamamoto, K, and Kadokawa, J-i (2015), "Acetylation of xanthan gum in ionic liquid" *Journal of Polymers and the Environment*, 23199-205.

Erdmann, R, Kabasci, S, and Heim, H-P (2021), "Thermal properties of plasticized cellulose acetate and its β-relaxation phenomenon" *Polymers*, 13(9), 1356.

Esa, F, Tasirin, SM, and Abd Rahman, N (2014), "Overview of bacterial cellulose production and application" *Agriculture and Agricultural Science Procedia*, 2113-119.

Fadel, SM, Hassan, ML, and Oksman, K (2013), "Improving tensile strength and moisture barrier properties of gelatin using microfibrillated cellulose" *Journal of Composite Materials*, 47(16), 1977-1985.

Fernandes, IdAA, Pedro, AC, Ribeiro, VR, Bortolini, DG, Ozaki, MSC, Maciel, GM, and Haminiuk, CWI (2020), "Bacterial cellulose: From production optimization to new applications" *International Journal of Biological Macromolecules*, 1642598-2611.

Ferrarezi, MMF, Rodrigues, GV, Felisberti, MI, and do Carmo Gonçalves, M (2013), "Investigation of cellulose acetate viscoelastic properties in different solvents and microstructure" *European Polymer Journal*, 49(9), 2730-2737.

Fischer, S, Thümmler, K, Volkert, B, Hettrich, K, Schmidt, I, and Fischer, K. Properties and applications of cellulose acetate. Macromolecular symposia, 2008. Wiley Online Library, 89-96.

Fordyce, C, and Meyer, I (1940), "Plasticizers for cellulose acetate and cellulose acetate butyrate" *Industrial & Engineering Chemistry*, 32(8), 1053-1060.

Fotie, G, Gazzotti, S, Ortenzi, MA, Limbo, S, and Piergiovanni, L (2023), "Performance comparison of coatings based on cellulose nanocrystals and microfibrillated cellulose for food packaging" *Carbohydrate Polymer Technologies and Applications*, 5100264.

French, AD, Bertoniere, NR, Battista, O, Cuculo, JA, and Gray, DG (2000), "Cellulose" *Kirk-Othmer Encyclopedia of Chemical Technology*.

Fritzler, B, Dharmavaram, S, Hartrim, R, and Diffendall, G (2014), "Acetic anhydride hydrolysis at high acetic anhydride to water ratios" *International Journal of Chemical Kinetics*, 46(3), 151-160.

Gao, Q, Lei, M, Zhou, K, Liu, X, Wang, S, and Li, H (2020), "Preparation of a microfibrillated cellulose/chitosan/polypyrrole film for Active Food Packaging" *Progress in Organic Coatings*, 149105907.

García Betancourt, ML, and Osorio-Aguilar, D-M (2022), Physicochemical Characterization of Nanocellulose: Composite, Crystallinity, Morphology. *Handbook of Nanocelluloses: Classification, Properties, Fabrication, and Emerging Applications.* Springer.

Godwin, AD (2017), 24 - Plasticizers. *In:* Kutz, M (ed.) *Applied Plastics Engineering Handbook (Second Edition).* William Andrew Publishing.

Gold, V (1948), "The hydrolysis of acetic anhydride" *Transactions of the Faraday Society*, 44506-518.

González, AG, and Herrador, MÁ (2007), "A practical guide to analytical method validation, including measurement uncertainty and accuracy profiles" *TrAC Trends in Analytical Chemistry*, 26(3), 227-238.

Hamid, SBA, Zain, SK, Das, R, and Centi, G (2016), "Synergic effect of tungstophosphoric acid and sonication for rapid synthesis of crystalline nanocellulose" *Carbohydrate Polymers*, 138349-355.

Harmon, JP, and Otter, R (2018), "Green chemistry and the search for new plasticizers" *ACS Sustainable Chemistry & Engineering*, 6(2), 2078-2085.

Harris, L, and Johnson, E (1933), "The production of strong, cellulose acetate films" *Review of Scientific Instruments*, 4(8), 454-455.

He, L, Song, F, Li, D-F, Zhao, X, Wang, X-L, and Wang, Y-Z (2020), "Strong and tough polylactic acid based composites enabled by simultaneous reinforcement and interfacial compatibilization of microfibrillated cellulose" *ACS Sustainable Chemistry & Engineering*, 8(3), 1573-1582.

Hoek, Z, du Toit, EL, Niemand, D, Wesley-Smith, J, and Focke, WW (2024), "Dried nanocellulose/xanthan as reinforcing fillers in thermoplastic starch" *Cellulose*, 31(11), 6733-6746.

Hoek, Z, Focke, W, and du Toit, E (2023) "Dried Xanthan Gum/Nanocellulose for Thermoplastic Starch Reinforcement", Paper submitted for consideration as a publication.

Huang, C, Yan, M, Wang, J, Shen, X, Wang, L, and Chen, Y (2012), "Synthesis of Composites with Microfibrillated Cellulose and Polylactic Acid" *Asian Journal of Chemistry*, 24(12).

Hussain, Z, Sajjad, W, Khan, T, and Wahid, F (2019), "Production of bacterial cellulose from industrial wastes: a review" *Cellulose*, 262895-2911.

Iwata, H, and Shimada, K (2012), Formulas, ingredients and production of cosmetics: technology of skin-and hair-care products in Japan, Springer Science & Business Media,

Jabbour, L, Gerbaldi, C, Chaussy, D, Zeno, E, Bodoardo, S, and Beneventi, D (2010), "Microfibrillated cellulose-graphite nanocomposites for highly flexible paper-like Li-ion battery electrodes" *Journal of Materials Chemistry*, 20(35), 7344-7347.

Jamaluddin, N, Kanno, T, Asoh, T-A, and Uyama, H (2019), "Surface modification of cellulose nanofiber using acid anhydride for poly (lactic acid) reinforcement" *Materials Today Communications*, 21100587.

Kargarzadeh, H, Mariano, M, Huang, J, Lin, N, Ahmad, I, Dufresne, A, and Thomas, S (2017), "Recent developments on nanocellulose reinforced polymer nanocomposites: A review" *Polymer*, 132368-393.

Katzbauer, B (1998), "Properties and applications of xanthan gum" *Polymer degradation and Stability*, 59(1-3), 81-84.

Kim, D, Le, NL, and Nunes, SP (2016), "The effects of a co-solvent on fabrication of cellulose acetate membranes from solutions in 1-ethyl-3-methylimidazolium acetate" *Journal of Membrane Science*, 520540-549.

Kim, JH, Lee, D, Lee, YH, Chen, W, and Lee, SY (2019), "Nanocellulose for energy storage systems: beyond the limits of synthetic materials" *Advanced Materials*, 31(20), 1804826.

Kim, SH, Lee, CM, and Kafle, K (2013), "Characterization of crystalline cellulose in biomass: Basic principles, applications, and limitations of XRD, NMR, IR, Raman, and SFG" *Korean Journal of Chemical Engineering*, 30(12), 2127-2141.

Kokol, V, Božič, M, Vogrinčič, R, and Mathew, AP (2015), "Characterisation and properties of homo-and heterogenously phosphorylated nanocellulose" *Carbohydrate Polymers*, 125301-313.

Kumar, V, Bollström, R, Yang, A, Chen, Q, Chen, G, Salminen, P, Bousfield, D, and Toivakka, M (2014), "Comparison of nano-and microfibrillated cellulose films" *Cellulose*, 213443-3456.

Li, K, McGrady, D, Zhao, X, Ker, D, Tekinalp, H, He, X, Qu, J, Aytug, T, Cakmak, E, Phipps, J, Ireland, S, Kunc, V, and Ozcan, S (2021), "Surface-modified and oven-dried microfibrillated cellulose reinforced biocomposites: Cellulose network enabled high performance" *Carbohydrate Polymers*, 256117525.

Li, W, Cai, G, and Zhang, P (2019), "A simple and rapid Fourier transform infrared method for the determination of the degree of acetyl substitution of cellulose nanocrystals" *Journal of Materials Science*, 54(10), 8047-8056.

Lu, J, and Drzal, LT (2010), "Microfibrillated cellulose/cellulose acetate composites: effect of surface treatment" *Journal of Polymer Science Part B: Polymer Physics*, 48(2), 153-161.

Matsuba, R, Kubota, H, and Matubayasi, N (2022), "All-atom molecular simulation study of cellulose acetate: amorphous structure and the dissolution of small molecule" *Cellulose*, 29(10), 5463-5478.

Miao, J, Yu, Y, Jiang, Z, and Zhang, L (2016), "One-pot preparation of hydrophobic cellulose nanocrystals in an ionic liquid" *Cellulose*, 231209-1219.

Mo, W, Kong, F, Chen, K, and Li, B (2022), "Relationship between freeze-drying and supercritical drying of cellulosic fibers with different moisture contents based on pore and crystallinity measurements" *Wood Science and Technology*, 56(3), 867-882.

Moelter, GM, and Schweizer, E (1949), "Heat Softening of Cellulose Acetate" *Industrial & Engineering Chemistry*, 41(4), 684-689.

Moniri, M, Boroumand Moghaddam, A, Azizi, S, Abdul Rahim, R, Bin Ariff, A, Zuhainis Saad, W, Navaderi, M, and Mohamad, R (2017), "Production and status of bacterial cellulose in biomedical engineering" *Nanomaterials*, 7(9), 257.

Nabili, A, Fattoum, A, Brochier-Salon, M-C, Bras, J, and Elaloui, E (2017), "Synthesis of cellulose triacetate-I from microfibrillated date seeds cellulose (Phoenix dactylifera L.)" *Iranian Polymer Journal*, 26137-147.

Nagarajan, K, Ramanujam, N, Sanjay, M, Siengchin, S, Surya Rajan, B, Sathick Basha, K, Madhu, P, and Raghav, G (2021), "A comprehensive review on cellulose nanocrystals and cellulose nanofibers: Pretreatment, preparation, and characterization" *Polymer Composites*, 42(4), 1588-1630.

Nakagaito, AN, and Yano, H (2004), "The effect of morphological changes from pulp fiber towards nano-scale fibrillated cellulose on the mechanical properties of high-strength plant fiber based composites" *Applied Physics A*, 78547-552.

Navale, AM, and Paranjape, AN (2016), "Glucose transporters: physiological and pathological roles" *Biophysical reviews*, 8(1), 5-9.

Nelson, ML, and O'Connor, RT (1964), "Relation of certain infrared bands to cellulose crystallinity and crystal latticed type. Part I. Spectra of lattice types I, II, III and of amorphous cellulose" *Journal of applied polymer science*, 8(3), 1311-1324.

Nelson, SJ, Creechley, JJ, Wale, ME, and Lujan, TJ (2020), "Print-A-Punch: A 3D printed device to cut dumbbell-shaped specimens from soft tissue for tensile testing" *Journal of Biomechanics*, 112110011.

Nigam, S, Das, AK, Matkawala, F, and Patidar, MK (2022), "An insight overview of bioplastics produced from cellulose extracted from plant material, its applications and degradation" *Environmental Sustainability*, 5(4), 423-441.

Nordenström, M, Kaldéus, T, Erlandsson, J, Pettersson, T, Malmstrom, E, and Wågberg, L (2021), "Redispersion strategies for dried cellulose nanofibrils" *ACS Sustainable Chemistry & Engineering*, 9(33), 11003-11010.

Ogura, K (2021), "Manufacturing Cellulose Nanofibers Using the Water Jet Method and Their Applications".

Okano, T, and Sarko, A (1984), "Mercerization of cellulose. I. X-ray diffraction evidence for intermediate structures" *Journal of applied polymer science*, 29(12), 4175-4182.

Omran, AAB, Mohammed, AA, Sapuan, S, Ilyas, R, Asyraf, M, Rahimian Koloor, SS, and Petrů, M (2021), "Micro-and nanocellulose in polymer composite materials: A review" *Polymers*, 13(2), 231.

Pääkkö, M, Ankerfors, M, Kosonen, H, Nykänen, A, Ahola, S, Österberg, M, Ruokolainen, J, Laine, J, Larsson, PT, and Ikkala, O (2007), "Enzymatic hydrolysis combined with mechanical shearing and high-pressure homogenization for nanoscale cellulose fibrils and strong gels" *Biomacromolecules*, 8(6), 1934-1941.

Pandey, A (2021), "Pharmaceutical and biomedical applications of cellulose nanofibers: a review" *Environmental Chemistry Letters*, 19(3), 2043-2055.

Peng, Y, Gardner, DJ, and Han, Y (2012a), "Drying cellulose nanofibrils: in search of a suitable method" *Cellulose*, 1991-102.

Peng, Y, Han, Y, and Gardner, DJ (2012b), "Spray-drying cellulose nanofibrils: Effect of drying process parameters on particle morphology and size distribution" *Wood and Fiber Science*, 448-461.

Phuong, VT, Verstiche, S, Cinelli, P, Anguillesi, I, Coltelli, M-B, and Lazzeri, A (2014), "Cellulose acetate blends-effect of plasticizers on properties and biodegradability" *Journal of Renewable Materials*, 2(1), 35-41.

Posada, P, Velásquez-Cock, J, Gómez-Hoyos, C, Serpa Guerra, AM, Lyulin, SV, Kenny, JM, Gañán, P, Castro, C, and Zuluaga, R (2020), "Drying and redispersion of plant cellulose nanofibers for industrial applications: a review" *Cellulose*, 27(18), 10649-10670.

Puls, J, Wilson, SA, and Hölter, D (2011), "Degradation of cellulose acetate-based materials: a review" *Journal of Polymers and the Environment*, 19152-165.

Qi, Y, Wang, S, Liza, AA, Li, J, Yang, G, Zhu, W, Song, J, Xiao, H, Li, H, and Guo, J (2023), "Controlling the nanocellulose morphology by preparation conditions" *Carbohydrate Polymers*, 319121146.

Ragab, MM, Othman, H, and Hassabo, AG (2024), "Utilization of regenerated cellulose fiber (banana fiber) in various textile applications and reinforced polymer composites" *Journal of Textiles, Coloration and Polymer Science*.

Rajendran, N, Runge, T, Bergman, RD, Nepal, P, Nair, N, and Ashraf, W (2025), "Economic and environmental impact analysis of cellulose nanofiber-reinforced concrete mixture production" *Resources, Conservation and Recycling*, 212107917.

Redlinger-Pohn, JD, Petkovšek, M, Gordeyeva, K, Zupanc, M, Gordeeva, A, Zhang, Q, Dular, M, and Soderberg, LD (2022), "Cavitation fibrillation of cellulose fiber" *Biomacromolecules*, 23(3), 847-862.

Rodrigues Filho, G, da Cruz, SF, Pasquini, D, Cerqueira, DA, de Souza Prado, V, and de Assunção, RMN (2000), "Water flux through cellulose triacetate films produced from heterogeneous acetylation of sugar cane bagasse" *Journal of Membrane Science*, 177(1-2), 225-231.

Roman, C, García-Morales, M, Eugenio, ME, Ibarra, D, Martín-Sampedro, R, and Delgado, MA (2021), "A sustainable methanol-based solvent exchange method to produce nanocellulose-based ecofriendly lubricants" *Journal of Cleaner Production*, 319128673.

Rudie, A (2017), "Commercialization of cellulose nanofibril (CNF) and cellulose nanocrystal (CNC): pathway and challenges" *Handbook of nanocellulose and cellulose nanocomposites*, 2761-797.

Rustemeyer, P. 1. History of CA and evolution of the markets. Macromolecular Symposia, 2004. Wiley Online Library, 1-6.

Saito, T, Hirota, M, Tamura, N, Kimura, S, Fukuzumi, H, Heux, L, and Isogai, A (2009), "Individualization of nano-sized plant cellulose fibrils by direct surface carboxylation using TEMPO catalyst under neutral conditions" *Biomacromolecules*, 10(7), 1992-1996.

Sassi, J-F, and Chanzy, H (1995), "Ultrastructural aspects of the acetylation of cellulose" *Cellulose*, 2111-127.

Serpa, A, Velásquez-Cock, J, Gañán, P, Castro, C, Vélez, L, and Zuluaga, R (2016), "Vegetable nanocellulose in food science: A review" *Food Hydrocolloids*, 57178-186.

Setyaningsih, D, Sadi, U, Muna, N, Isroi, I, Suryawan, N, and Nurfauzi, A (2018), "Cellulose nanofiber isolation from palm oil Empty Fruit Bunches (EFB) through strong acid hydrolysis" *IOP Conference Series: Earth and Environmental Science*, 141012027.

Shaaban, E (2015), "What are all possible reasons for the peak shift in X-Ray Diffraction?".

Silva, LE, dos Santos, AdA, Torres, L, McCaffrey, Z, Klamczynski, A, Glenn, G, Sena Neto, ARd, Wood, D, Williams, T, Orts, W, Damásio, RAP, and Tonoli, GHD (2021), "Redispersion and structural change evaluation of dried microfibrillated cellulose" *Carbohydrate Polymers*, 252117165.

Sinquefield, S, Ciesielski, PN, Li, K, Gardner, DJ, and Ozcan, S (2020), "Nanocellulose dewatering and drying: current state and future perspectives" *ACS Sustainable Chemistry & Engineering*, 8(26), 9601-9615.

Sofla, MSK, Mortazavi, S, and Seyfi, J (2020), "Preparation and characterization of polyvinyl alcohol/chitosan blends plasticized and compatibilized by glycerol/polyethylene glycol" *Carbohydrate Polymers*, 232115784.

Somerville, C (2006), "Cellulose synthesis in higher plants" *Annu. Rev. Cell Dev. Biol.*, 22(1), 53-78.

Spence, KL, Venditti, RA, Rojas, OJ, Habibi, Y, and Pawlak, JJ (2011), "A comparative study of energy consumption and physical properties of microfibrillated cellulose produced by different processing methods" *Cellulose*, 181097-1111.

Stenstad, P, Andresen, M, Tanem, BS, and Stenius, P (2008), "Chemical surface modifications of microfibrillated cellulose" *Cellulose*, 1535-45.

Sun, L-H, Ounaies, Z, Gao, X-L, Whalen, CA, and Yang, Z-G (2011), "Preparation, characterization, and modeling of carbon nanofiber/epoxy nanocomposites" *Journal of Nanomaterials*, 2011(1), 307589.

Syverud, K, and Stenius, P (2009), "Strength and barrier properties of MFC films" *Cellulose*, 1675-85.

Tahiri, C, and Vignon, MR (2000), "TEMPO-oxidation of cellulose: Synthesis and characterisation of polyglucuronans" *Cellulose*, 7177-188.

Tardy, BL, Yokota, S, Ago, M, Xiang, W, Kondo, T, Bordes, R, and Rojas, OJ (2017), "Nanocellulose–surfactant interactions" *Current Opinion in Colloid & Interface Science*, 2957-67.

Teixeira, SC, Silva, RRA, de Oliveira, TV, Stringheta, PC, Pinto, MRMR, and Soares, NdFF (2021), "Glycerol and triethyl citrate plasticizer effects on molecular, thermal, mechanical, and barrier properties of cellulose acetate films" *Food Bioscience*, 42101202.

Thompson, L, Azadmanjiri, J, Nikzad, M, Sbarski, I, Wang, J, and Yu, A (2019), "Cellulose nanocrystals: production, functionalization and advanced applications" *Reviews on Advanced Materials Science*, 58(1), 1-16.

Tian, J, Cao, Z, Qian, S, Xia, Y, Zhang, J, Kong, Y, Sheng, K, Zhang, Y, Wan, Y, and Takahashi, J (2022), "Improving tensile strength and impact toughness of plasticized poly(lactic acid) biocomposites by incorporating nanofibrillated cellulose" *Nanotechnology Reviews*, 11(1), 2469-2482.

Trache, D, Tarchoun, AF, Derradji, M, Hamidon, TS, Masruchin, N, Brosse, N, and Hussin, MH (2020), "Nanocellulose: From Fundamentals to Advanced Applications" *Frontiers in Chemistry*, 8.

Trivedi, MK, Nayak, G, Patil, S, Tallapragada, RM, and Mishra, R (2015), "Impact of biofield treatment on chemical and thermal properties of cellulose and cellulose acetate" *Journal of Bioengineering & Biomedical Science*, 5(3).

Tucker III, CL, and Liang, E (1999), "Stiffness predictions for unidirectional short-fiber composites: Review and evaluation" *Composites science and technology*, 59(5), 655-671.

Turbak, AF, Snyder, FW, and Sandberg, KR. Microfibrillated cellulose, a new cellulose product: properties, uses, and commercial potential. J Appl Polym Sci Appl Polym Symp, 1983. 815-827.

Vatanpour, V, Pasaoglu, ME, Barzegar, H, Teber, OO, Kaya, R, Bastug, M, Khataee, A, and Koyuncu, I (2022), "Cellulose acetate in fabrication of polymeric membranes: A review" *Chemosphere*, 295133914.

Venkatarajan, S, and Athijayamani, A (2021), "An overview on natural cellulose fiber reinforced polymer composites" *Materials Today: Proceedings*, 373620-3624.

Wang, B, Sain, M, and Oksman, K (2007), "Study of structural morphology of hemp fiber from the micro to the nanoscale" *Applied Composite Materials*, 1489-103.

Wang, Q, Ji, C, Sun, J, Zhu, Q, and Liu, J (2020), "Structure and properties of polylactic acid biocomposite films reinforced with cellulose nanofibrils" *Molecules*, 25(14), 3306.

Wang, Q, and Zhu, J (2016), "Effects of mechanical fibrillation time by disk grinding on the properties of cellulose nanofibrils" *Tappi J*, 15(6), 419-423.

Ward, K (1950), "Crystallinity of Cellulose and Its Significance for the Fiber Properties" *Textile Research Journal*, 20(6), 363-372.

Wertz, J-L, Bédué, O, and Mercier, JP (2010), Cellulose science and technology, EPFL press,

Winston, PW, and Bates, DH (1960), "Saturated Solutions For the Control of Humidity in Biological Research" *Ecology*, 41(1), 232-237.

Wypych, G (2004), "Plasticizers use and selection for specific polymers" *Handbook of plasticizers*, 1.

Xhanari, K, Syverud, K, Chinga-Carrasco, G, Paso, K, and Stenius, P (2011), "Reduction of water wettability of nanofibrillated cellulose by adsorption of cationic surfactants" *Cellulose*, 18257-270.

Xu, R-M, Yang, T-T, Vidović, E, Jia, R-N, Zhang, J-M, Mi, Q-Y, and Zhang, J (2020), "Cellulose acetate thermoplastics with high modulus, dimensional stability and anti-migration properties by using CA-g-PLA as macromolecular plasticizer" *Chinese Journal of Polymer Science*, 381141-1148.

Xu, Y, Xu, Y, Chen, H, Gao, M, Yue, X, and Ni, Y (2022), "Redispersion of dried plant nanocellulose: A review" *Carbohydrate Polymers*, 119830.

Yadav, N, and Hakkarainen, M (2021), "Degradable or not? Cellulose acetate as a model for complicated interplay between structure, environment and degradation" *Chemosphere*, 265128731.

Yetiş, F, Liu, X, Sampson, WW, and Gong, RH (2020), "Acetylation of lignin containing microfibrillated cellulose and its reinforcing effect for polylactic acid" *European Polymer Journal*, 134109803.

Yi, T, Zhao, H, Mo, Q, Pan, D, Liu, Y, Huang, L, Xu, H, Hu, B, and Song, H (2020), "From Cellulose to Cellulose Nanofibrils—A Comprehensive Review of the Preparation and Modification of Cellulose Nanofibrils" *Materials*, 13(22), 5062.

Zaaba, NF, Jaafar, M, and Ismail, H (2021), "Tensile and morphological properties of nanocrystalline cellulose and nanofibrillated cellulose reinforced PLA bionanocomposites: A review" *Polymer Engineering & Science*, 61(1), 22-38.

Zhai, L, Kim, HC, Kim, D, Muthoka, RM, and Kim, J (2018), "Young's moduli of cellulose nanofibers measured by atomic force microscopy" *Nano-, Bio-, Info-Tech Sensors, and 3D Systems II*, 10597104-107.

Zhao, N, Li, Q, and Park, CB (2015), "Foaming of poly(vinyl alcohol)/microfibrillated cellulose composites" *Huagong Xuebao/CIESC Journal*, 66(2), 806-813.

Zhou, H, Tong, H, Lu, J, Cheng, Y, Qian, F, Tao, Y, and Wang, H (2021), "Preparation of bio-based cellulose acetate/chitosan composite film with oxygen and water resistant properties" *Carbohydrate Polymers*, 270118381.

Zhou, M, Fan, M, Zhao, Y, Jin, T, and Fu, Q (2016), "Effect of stretching on the mechanical properties in melt-spun poly(butylene succinate)/microfibrillated cellulose (MFC) nanocomposites" *Carbohydrate Polymers*, 140383-392.

Zinge, C, and Kandasubramanian, B (2020), "Nanocellulose based biodegradable polymers" *European Polymer Journal*, 133109758.

7 Appendices

7.1 Appendix A: DS Calculation

	DS (%)				
	0	0.5	1	1.5	2
Baseline Area (1158 cm^{-1})	9.2703	11.1522	18.4206	6.3675	13.8848
Measure Area(1744 cm^{-1})	0.178895	0.7366	1.6128	0.8825	2.2628
Relative Area	0.267944	0.917088	1.215672	1.924356	2.2628
Corrected DS	0	0.649144	0.947728	1.656412	1.994856
Target DS	0	0.5	1	1.5	2
Variance(Corrected/Target)	**-**	**1.298287**	**0.947728**	**1.104275**	**0.997428**

7.2 Appendix B: Modulus of elasticity of films (MPa)

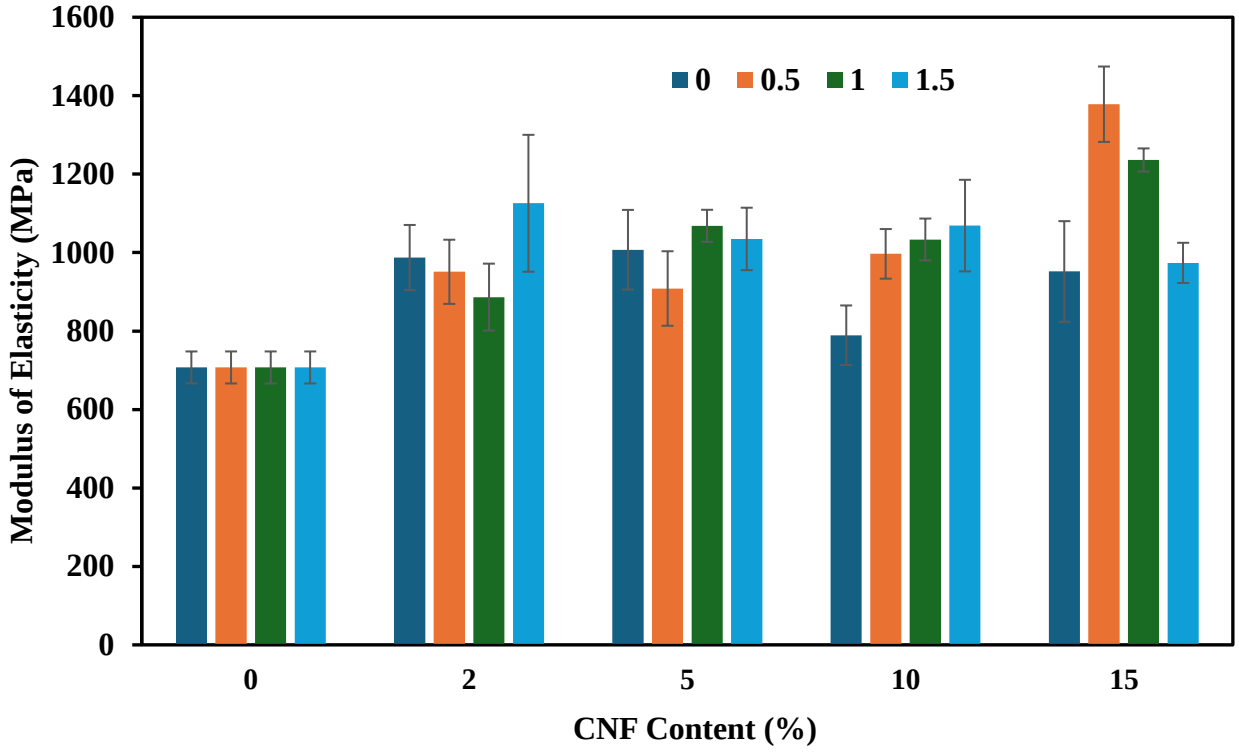

7.3 Appendix B: Tensile strength of films (MPa)

CNF Content (%)	Degree of Substitution			
	0	0.5	1	1.5
0	36.2 ± 5.9			
2	43.2 ± 5.2	42.4 ± 4.07	43.18 ± 3.59	53.38 ± 10.5
5	45.8 ± 3.7	39.04 ± 3.93	45.1 ± 1.75	41.2 ± 1.8
10	39.3 ± 3.6	40.53 ± 2.3	40.41 ± 1.8	41.3 ± 2.77
15	53.6 ± 2.7	46.98 ± 2.95	45.52 ± 3.07	43.4 ± 2.6